

Theory and Fast Learned Solver for ℓ^1 -TV Regularization

Xinling Liu*

Jianjun Wang[†]

Bangti Jin[‡]

December 5, 2024

Abstract

The ℓ^1 and total variation (TV) penalties have been used successfully in many areas, and the combination of the ℓ^1 and TV penalties can lead to further improved performance. In this work, we investigate the mathematical theory and numerical algorithms for the ℓ^1 -TV model in the context of signal recovery: we derive the sample complexity of the ℓ^1 -TV model for recovering signals with sparsity and gradient sparsity. Also we propose a novel algorithm (PGM-ISTA) for the regularized ℓ^1 -TV problem, and establish its global convergence and parameter selection criteria. Furthermore, we construct a fast learned solver (LPGM-ISTA) by unrolling PGM-ISTA. The results for the experiment on ECG signals show the superior performance of LPGM-ISTA in terms of recovery accuracy and computational efficiency.

Keywords. ℓ^1 -TV regularization; sample complexity; learned solver; algorithm unrolling.

1 Introduction

In the last two decades, compressed sensing (CS) has achieved remarkable successes since the pioneering work of Candès, Donoho, Romberg, and Tao [11, 20]. So far, it has found applications in many fields, e.g., magnetic resonance imaging [40], single-pixel imaging [22] and nonlinear parameter identification [31]. The classical setup is to reconstruct an unknown sparse signal $\mathbf{x}^* \in \mathbb{R}^n$ from linear measurements of the form

$$\mathbf{y} = \mathbf{A}\mathbf{x}^* + \mathbf{e}, \quad (1.1)$$

where $\mathbf{A} \in \mathbb{R}^{m \times n}$ ($m \ll n$) is a known sensing matrix and $\mathbf{e} \in \mathbb{R}^m$ denotes noise. Problem (1.1) is ill-posed, and the key to address the ill-posedness is to suitably exploit prior structure of real-world signals so as to constrain the solution space. Typical examples include signal sparsity and gradient sparsity, which may appear simultaneously in many real-world datasets. This study aims to build a mathematical theory and numerical algorithms of one method for recovering such signals.

First we briefly review single sparsity or gradient sparsity, respectively. When the signal is sparse, many mathematical models based on (1.1) have been proposed, e.g., ℓ^1 minimization [21, 55], ℓ^p ($0 \leq p < 1$) minimization [58, 28, 30] and general nonconvex minimization [56, 29]. One of the most popular models is the following ℓ^1 minimization:

$$(\ell^1): \quad \min_{\mathbf{x} \in \mathbb{R}^n} \|\mathbf{x}\|_1, \quad \text{s.t.} \quad \|\mathbf{A}\mathbf{x} - \mathbf{y}\|_2 \leq \epsilon, \quad (1.2)$$

where $\epsilon \geq 0$ denotes noise level (i.e. $\|\mathbf{e}\|_2 \leq \epsilon$). If \mathbf{x}^* is s -sparse (i.e. $\|\mathbf{x}^*\|_0 \leq s$, where $\|\mathbf{x}^*\|_0$ denotes the number of nonzero entries of \mathbf{x}^*) and \mathbf{A} satisfies certain properties (e.g., null sparse property and restricted isometry property), then \mathbf{x}^* can be effectively recovered from a few measurements by, e.g., orthogonal matching pursuit (OMP) [41, 59] and iterative shrinkage-threshold algorithm (ISTA) [19] or its fast version (FISTA) [6]. Signals with few details are often locally constant with a few jumps, which can be well represented as sparse gradients [27, 39]. A signal \mathbf{x}^* with sparse gradients takes the form of a sparse $\mathbf{D}\mathbf{x}^*$ (with $\mathbf{D} = \text{circ}([-1, 1, 0, \dots, 0]) \in \mathbb{R}^{(n-1) \times n}$ denoting a row circulant difference matrix). One popular approach to recover such \mathbf{x}^* is to solve

$$(\text{TV}): \quad \min_{\mathbf{x} \in \mathbb{R}^n} \|\mathbf{x}\|_{\text{TV}}, \quad \text{s.t.} \quad \|\mathbf{A}\mathbf{x} - \mathbf{y}\|_2 \leq \epsilon, \quad (1.3)$$

where $\|\mathbf{x}\|_{\text{TV}} = \|\mathbf{D}\mathbf{x}\|_1$ denotes the total variation (TV) seminorm of \mathbf{x} . Cai et al. [9] proved that the TV method can recover a gradient s -sparse signal \mathbf{x}^* (i.e., $\|\mathbf{D}\mathbf{x}^*\|_0 \leq s$) if the sampling number m obeys

*School of Mathematics & Statistics, Southwest University, Chongqing 400715, China and Key Laboratory of Optimization Theory and Applications at China West Normal University of Sichuan Province, School of Mathematics and Information, China West Normal University, Nanchong 637009, China (fsluixl@163.com)

[†]School of Mathematics & Statistics, Southwest University, Chongqing 400715, China (wj@swu.edu.cn, Corresponding author)

[‡]Department of Mathematics, The Chinese University of Hong Kong, Shatin, New Territories, Hong Kong, China (bangti.jin@gmail.com, b.jin@cuhk.edu.hk)

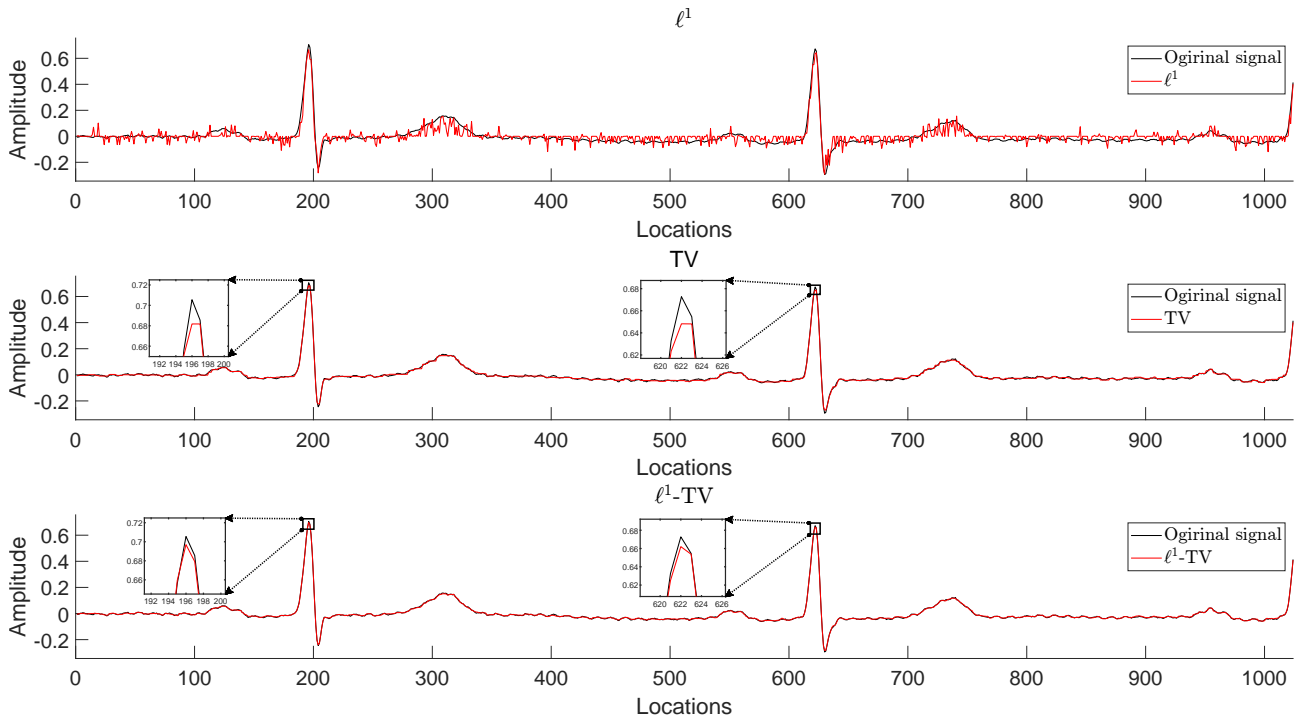


Figure 1: The comparison of ℓ^1 , TV and ℓ^1 -TV under Gaussian sampling with a sampling ratio of 0.5.

$m = \mathcal{O}(\sqrt{sn} \ln n)$ and the entries of \mathbf{A} follow the standard Gaussian distribution. However, the bound is not optimal, and several works have improved the result [17, 18, 24, 25]. The TV problem (1.3) can be effectively solved using, e.g., proximal gradient descent algorithm and projected subgradient algorithm [5].

The use of the ℓ^1 and TV penalties promotes respectively sparsity and gradient sparsity in the signals. However, one single penalty cannot well characterize signals with both properties, e.g., electrocardiogram (ECG) signals [23] and time-varying signals [2]. Tibshirani et al. [51] proposed to combine the ℓ^1 and TV penalties to promote sparsity in both signals and their successive differences, which has achieved great success in many applications [50, 16, 42, 54, 61], e.g., regression, feature selection and denoising. However, it has not been studied in the context of CS so far. This motivated the theoretical study of the following problem:

$$(\ell^1\text{-TV}) : \quad \min_{\mathbf{x} \in \mathbb{R}^n} \lambda_1 \|\mathbf{x}\|_1 + \lambda_2 \|\mathbf{x}\|_{\text{TV}}, \quad \text{s.t.} \quad \|\mathbf{A}\mathbf{x} - \mathbf{y}\|_2 \leq \epsilon, \quad (1.4)$$

where regularization parameters $\lambda_1 \geq 0$ and $\lambda_2 \geq 0$. Obviously, if $\lambda_1 = 0$ and $\lambda_2 > 0$, (1.4) reduces to (1.2), and if $\lambda_1 > 0$ and $\lambda_2 = 0$, (1.4) becomes (1.3). To illustrate the benefit of the ℓ^1 -TV method, we take one ECG signal from the MIT-BIH Arrhythmia Database [44] as the original signal and apply random Gaussian sampling with a ratio of 0.5 and $\epsilon = 0$. The restorations by the ℓ^1 , TV and ℓ^1 -TV methods are shown in Fig. 1, which shows that the restorations by the ℓ^1 and TV methods are unsatisfactory, whereas ℓ^1 -TV gives a very satisfactory reconstruction. Thus, the ℓ^1 -TV model can enforce sparsity in both signals and the differences between consecutive components of the signals in the CS framework. To theoretically substantiate this empirical observation, we shall establish the required sampling number for the robust recovery of signals regarding given sparsity and gradient sparsity levels.

The second important issue is the algorithmic aspect of the model (1.4). The model (1.4) poses big challenges to the numerical solution since it involves both non-separable term $\|\mathbf{x}\|_{\text{TV}}$ and non-smooth term $\|\mathbf{x}\|_1$, as well as quadratic inequality constraint. Li et al. [36] suggested a level-set method for solving (1.4), which however can be computationally very challenging due to the complicated geometry of the quadratic inequality constraint, and the potentially unknown noise level. In this work, we consider the regularized model

$$\min_{\mathbf{x} \in \mathbb{R}^n} \frac{1}{2} \|\mathbf{y} - \mathbf{A}\mathbf{x}\|_2^2 + \lambda_1 \|\mathbf{x}\|_1 + \lambda_2 \|\mathbf{D}\mathbf{x}\|_1, \quad (1.5)$$

by slightly abusing the notation λ_1 and λ_2 . Note that such a strategy is common in the community, and there are several works on the equivalence between the constrained problem and its regularized counterpart [34, 3, 60]. Transforming problem (1.4) to (1.5) avoids the need to estimate the noise level ϵ and facilitates implementing existing algorithms, e.g., linearized alternating direction method of multipliers (LADMM) [35] and smooth-FISTA (S-FISTA) [7].

To circumvent these issues, we develop an algorithm unrolling approach for problem (1.5) such that all algorithmic hyper-parameters in the corresponding algorithm (not including the regularization parameters λ_1

and λ_2) are learnable. Algorithm unrolling is a powerful technique: it inherits the interpretability of iterative algorithms and high expressivity of deep neural networks [43]. Since its first introduction by Gregor et al. [26], the idea has found many successful applications, e.g., signal and imaging processing, including compressed sensing [62], sparse coding [26] and tomographic reconstruction [4]; see the review [43] for details. In algorithm unrolling, each iteration typically corresponds to one layer of a neural network, and the employed operator must be adapted to the activation function used by the neural network. For example, in ISTA (for the ℓ^1 minimization), the soft-threshold operator is the activation function in learned ISTA (LISTA) [26]. Similarly, the 1D TV minimization can also be effectively unfolded into a recurrent neural network (i.e., LPGD-Taut) [14]. These works motivate developing an algorithm unrolling approach for solving problem (1.5). However, due to the presence of two penalties, directly applying these important findings to (1.5) is infeasible. We shall develop a novel fast learned solver for (1.5) by unrolling a new algorithm with guaranteed global convergence and rigorous parameter selection criteria.

The main contributions of the work are as follows.

- We present novel theoretical guarantees on the robust recovery via (1.4). The bound on the sampling number reflects the joint influence of sparsity and gradient sparsity of the signal, where higher levels of sparsity or gradient sparsity result in a larger sampling number.
- We propose a novel algorithm, i.e., proximal gradient mapping ISTA (PGM-ISTA) for solving (1.5), and prove its global convergence and parameter selection. Furthermore, we develop an efficient learned solver LPGM-ISTA for the model (1.5) based on algorithm unrolling.
- We conduct extensive numerical experiments, including ECG signals. The results show that LPGM-ISTA already perform very well with only 2 layers/iterations, and outperforms traditional algorithms in terms of computing time and accuracy.

Lastly, we situate the present work in existing works. First, in the analysis, to obtain the robust recovery guarantee of the ℓ^1 -TV method, we select a vector from the subdifferential of the objective function in (1.4) that yields an upper bound on its statistical dimension, and then derive a bound on the sampling number for successful signal recovery. Several studies [10, 32, 33, 24] have addressed closely related topics. These studies can provide recovery guarantee for the model (1.4), but they focus on analysis sparsity, and thus do not deliver the sampling number for the sparsity and gradient sparsity levels of the concerned signal. Second, PGM-ISTA is based on proximal operator and gradient mapping operator [5], which directly solves problem (1.5), rather than its equivalent or approximate alternatives. Thus, PGM-ISTA may have a lower computational complexity per iteration, compared to LADMM [35], which requires the update of auxiliary variables. Moreover, the S-FISTA [7] is an approximate approach for solving problem (1.5), and its performance depends heavily on the smoothing parameter. Traditional optimization algorithms for problem (1.5) are often time-consuming since they require many iterations (dozens to hundreds). The unrolled network LPGM-ISTA provides an efficient way to tackle the computational challenge.

The rest of this paper is structured as follows. In Section 2, we recall useful notation, and some technical lemmas, and in Section 3, present the robust guarantee for the ℓ^1 -TV method (1.4). In Section 4, we propose a learned solver by unrolling the PGM-ISTA algorithm, and in Section 5, provide numerical illustrations. All the proofs are given in Section 6. We conclude in Section 7 with additional discussions.

2 Preliminaries

First we recall useful notation. Throughout, scalars are denoted by lowercase case letters (e.g. x), vectors by bold lowercase letters (e.g. \mathbf{x}), and matrices by bold uppercase letters (e.g. \mathbf{A}). The i -th element of a vector \mathbf{x} is denoted by x_i or $[\mathbf{x}]_i$. $\mathbf{0}$ denotes a zero vector, and \mathbf{I}_n the identity matrix of size $n \times n$. We denote sets by hollow capitalized letters (e.g. \mathbb{S}), and denote by $|\mathbb{S}|$ its cardinality. \mathbb{N}_+ refers to the set of positive integers, and $[n] = \{1, 2, \dots, n\}$ and \mathbb{S}^c the complement of \mathbb{S} . For a vector $\mathbf{x} \in \mathbb{R}^n$, $\mathbf{x}_{\mathbb{S}}$ is the vector in \mathbb{R}^n that coincides with \mathbf{x} on the entries in \mathbb{S} and zero otherwise. For a vector $\mathbf{x} \in \mathbb{R}^n$ and $p > 0$, we denote $\|\mathbf{x}\|_p = (\sum_{i=1}^n |x_i|^p)^{1/p}$ as the ℓ^p norm of \mathbf{x} , and we also denote $\|\mathbf{x}\|_0 = |\{i : x_i \neq 0\}|$. For a matrix \mathbf{A} , we denote its spectral norm by $\|\mathbf{A}\|_2$. For any $\mathbf{x} \in \mathbb{R}^n$ and a set $\mathbb{S} \subset \mathbb{R}^n$, we denote the distance of \mathbf{x} and \mathbb{S} by $\text{dist}(\mathbf{x}, \mathbb{S}) = \min_{\mathbf{z} \in \mathbb{S}} \|\mathbf{x} - \mathbf{z}\|_2$. The operator $[a]_+ = \max\{a, 0\}$ gives the positive part of the scalar a . For $\mathbf{x}, \mathbf{y} \in \mathbb{R}^n$, $\mathbf{x} \odot \mathbf{y}$ denotes the Hadamard / componentwise product. We denote the support of $\mathbf{x} \in \mathbb{R}^n$ by $\mathbb{S}_R(\mathbf{x}) := \{i \in [n] : x_i \neq 0\}$ (\mathbb{S}_R for short) and the gradient support by $\mathbb{S}_G(\mathbf{x}) := \{i \in [n-1] : x_{i+1} - x_i \neq 0\}$ (\mathbb{S}_G for short). We denote by \mathbb{S}^* the set of solutions to problem (1.5).

First we recall the definitions of descent cone, subdifferential, and statistical dimension. Recall that a proper convex function takes at least one finite value but never the value $-\infty$. We denote the set of extended real numbers by $\overline{\mathbb{R}} = \mathbb{R} \cup \{\pm\infty\}$.

Definition 2.1 ([52]). Let $g : \mathbb{R}^n \rightarrow \overline{\mathbb{R}}$ be a proper convex function. The descent cone $\mathcal{D}(g, \mathbf{x})$ of the function g at a point $\mathbf{x} \in \mathbb{R}^n$ is defined by

$$\mathcal{D}(g, \mathbf{x}) = \bigcup_{t>0} \{\mathbf{u} \in \mathbb{R}^n : g(\mathbf{x} + t\mathbf{u}) \leq g(\mathbf{x})\}.$$

Definition 2.2 ([47]). The subdifferential of a convex function $f : \mathbb{R}^n \rightarrow \mathbb{R}$ at a point $\mathbf{x} \in \mathbb{R}^n$ is given by $\partial f(\mathbf{x}) = \{\mathbf{z} \in \mathbb{R}^n : f(\mathbf{y}) \geq f(\mathbf{x}) + \langle \mathbf{z}, \mathbf{y} - \mathbf{x} \rangle, \forall \mathbf{y} \in \mathbb{R}^n\}$.

Definition 2.3 ([47]). For a given non-empty set $\mathbb{K} \subset \mathbb{R}^n$, the cone obtained by \mathbb{K} is defined by $\text{cone}(\mathbb{K}) = \{\lambda \mathbf{x} \in \mathbb{R}^n, \mathbf{x} \in \mathbb{K}, \lambda \geq 0\}$.

Definition 2.4 ([1]). Let $\mathbb{K} \subset \mathbb{R}^n$ be a convex closed cone and $\mathbf{g} \sim \mathcal{N}(\mathbf{0}, \mathbf{I}_n)$ be a standard Gaussian vector in \mathbb{R}^n . The statistical dimension of \mathbb{K} is defined by

$$\delta(\mathbb{K}) = \mathbb{E}[\text{dist}^2(\mathbf{g}, \mathbb{K}^\circ)] = \min_{\mathbf{x} \in \mathbb{K}^\circ} \|\mathbf{g} - \mathbf{x}\|_2, \quad (2.1)$$

where $\mathbb{E}[\cdot]$ denotes the operator for expectation and $\mathbb{K}^\circ = \{\mathbf{z} \in \mathbb{R}^n : \langle \mathbf{z}, \mathbf{v} \rangle \leq 0 \forall \mathbf{v} \in \mathbb{K}\}$ denotes the set of outward normals of \mathbb{K} , i.e., the polar cone of \mathbb{K} .

The descent cone is connected with the subdifferential by [47]

$$[\mathcal{D}(g, \mathbf{x})]^\circ = \text{cone}(\partial g(\mathbf{x})) = \bigcup_{t \geq 0} \{t\mathbf{z} : \mathbf{z} \in \partial g(\mathbf{x})\}. \quad (2.2)$$

Combining (2.1) and (2.2) gives

$$\begin{aligned} \delta(\mathcal{D}(g, \mathbf{x})) &= \mathbb{E}[\text{dist}^2(\mathbf{g}, \mathcal{D}(g, \mathbf{x})^\circ)] = \mathbb{E}[\text{dist}^2(\mathbf{g}, \text{cone}(\partial g(\mathbf{x})))] \\ &= \mathbb{E} \left[\inf_{\substack{t \geq 0 \\ \mathbf{z} \in \partial g(\mathbf{x})}} \|\mathbf{g} - t\mathbf{z}\|_2^2 \right]. \end{aligned} \quad (2.3)$$

Next, we give the definition of conic Gaussian width and its relation with statistical dimension.

Definition 2.5 ([52]). Let \mathbb{S}^{n-1} be the $(n-1)$ -dimensional unit sphere, and $\mathbb{K} \subset \mathbb{R}^n$ be a cone, not necessarily convex. The conic Gaussian width $w(\mathbb{K})$ is defined by

$$w(\mathbb{K}) = \mathbb{E} \left[\sup_{\mathbf{u} \in \mathbb{K} \cap \mathbb{S}^{n-1}} \langle \mathbf{g}, \mathbf{u} \rangle \right]. \quad (2.4)$$

The conic Gaussian width is useful for estimating the sampling number m .

Lemma 2.1 ([1, Proposition 10.2]). Let \mathbb{K} be a convex cone. Then the statistical dimension $\delta(\mathbb{K})$ and the conic Gaussian width $w(\mathbb{K})$ satisfy

$$w^2(\mathbb{K}) \leq \delta(\mathbb{K}) \leq w^2(\mathbb{K}) + 1. \quad (2.5)$$

Combining (2.3) with Lemma 2.1 gives

$$w^2(\mathcal{D}(g, \mathbf{x})) \leq \mathbb{E} \left[\inf_{\substack{t \geq 0 \\ \mathbf{z} \in \partial g(\mathbf{x})}} \|\mathbf{g} - t\mathbf{z}\|_2^2 \right]. \quad (2.6)$$

Definition 2.6 ([5, Definition 5.1]). Fix $l \geq 0$. A function $f : \mathbb{R}^n \rightarrow (-\infty, \infty]$ is said to be l -smooth over a set $\mathbb{K} \subset \mathbb{R}^n$ if it is differentiable over \mathbb{K} and satisfies $\|\nabla f(\mathbf{x}) - \nabla f(\mathbf{y})\|_2 \leq l\|\mathbf{x} - \mathbf{y}\|_2$ for all $\mathbf{x}, \mathbf{y} \in \mathbb{K}$, and the constant l is called the smoothness parameter.

Definition 2.7 ([5, Definition 6.1]). For the function $f : \mathbb{K} \rightarrow (-\infty, \infty]$, the proximal mapping of f at $\mathbf{x} \in \mathbb{K}$ is the operator given by

$$\text{prox}_f(\mathbf{x}) = \arg \min_{\mathbf{u} \in \mathbb{K}} f(\mathbf{u}) + \frac{1}{2}\|\mathbf{u} - \mathbf{x}\|_2^2.$$

For $f(\mathbf{x}) = \lambda_1 \|\mathbf{x}\|_1$, the proximal mapping is given by the soft threshold operator:

$$\mathcal{S}_{\lambda_1}(\mathbf{x}) := \text{prox}_f(\mathbf{x}) = \text{sign}(\mathbf{x}) \odot \max\{0, |\mathbf{x}| - \lambda_1\}, \quad (2.7)$$

For $f(\mathbf{x}) = \lambda_2 \|\mathbf{x}\|_{\text{TV}}$, we denote $\mathcal{T}_{\lambda_2}(\mathbf{x}) := \text{prox}_f(\mathbf{x})$. It can be computed via dynamic programming, e.g., taut-string algorithm [15] at an $\mathcal{O}(n)$ complexity. Thus, $\mathcal{P}_{\lambda_1}^{\lambda_2}(\mathbf{x}) = \text{prox}_g(\mathbf{x})$ can be computed efficiently.

Lemma 2.2 ([38, Theorem 1]). Let $\mathbf{x} \in \mathbb{R}^n$ and $g(\mathbf{x}) = \lambda_1 \|\mathbf{x}\|_1 + \lambda_2 \|\mathbf{x}\|_{\text{TV}}$. Then there holds

$$\mathcal{P}_{\lambda_1}^{\lambda_2}(\mathbf{x}) := \text{prox}_g(\mathbf{x}) = \mathcal{S}_{\lambda_1}(\mathcal{T}_{\lambda_2}(\mathbf{x})).$$

3 Recovery guarantee for ℓ^1 -TV regularization

Now we provide robust recovery guarantee of the model (1.4). We first give Theorem 3.1 for estimating the statistical dimension $\delta(\mathcal{D}(g, \mathbf{x}))$ of $\mathcal{D}(g, \mathbf{x})$. It is crucial for proving Theorem 3.2 on robust recovery. Below we denote the regular sparsity by $s_r(\mathbf{x}) = |\mathbb{S}_R(\mathbf{x})|$ (s_r for short), and the gradient sparsity by $s_g(\mathbf{x}) = |\mathbb{S}_G(\mathbf{x})|$ (s_g for short). All the proofs are given in Section 6.1.

Theorem 3.1. *Let $n \in \mathbb{N}_+$, $\mathbf{x} \in \mathbb{R}^n$, and $s_r = |\mathbb{S}_R|$, $s_g = |\mathbb{S}_G|$. Then we have*

$$\delta(\mathcal{D}(g, \mathbf{x})) \leq \Phi(s_r, s_g), \quad (3.1)$$

with

$$\Phi(s_r, s_g) = n - \frac{6}{\pi} \frac{[\lambda_1(n - s_r) + \sqrt{2}\lambda_2(n - 1 - s_g)]^2}{3n\lambda_1^2 + 4(2n + s_g - 4)\lambda_2^2 + 12\lambda_1\lambda_2 \min\{s_r, s_g\}}. \quad (3.2)$$

Remark 1. *Theorem 3.1 gives an upper bound on $\delta(\mathcal{D}(g, \mathbf{x}))$, which is crucial for the recovery guarantee of (1.4). By Lemma 2.1 and the estimate (2.6), we can bound the conic Gaussian width of $\mathcal{D}(g, \mathbf{x})$ by*

$$w^2(\mathcal{D}(g, \mathbf{x})) \leq \delta(\mathcal{D}(g, \mathbf{x})) \leq \Phi(s_r, s_g). \quad (3.3)$$

If $\lambda_1 = 0$, the ℓ^1 -TV method reduces to the TV method, and (3.3) implies

$$w^2(\mathcal{D}(\|\cdot\|_{\text{TV}}, \mathbf{x})) \leq \Phi(s_r, s_g) = n - \frac{3}{\pi} \frac{(n - s_g - 1)^2}{2n + s_g - 4} \triangleq \Phi_{\text{TV}},$$

which is identical with that in [17, Theorem 1] for the TV method. If $\lambda_2 = 0$, the ℓ^1 -TV method reduces to the ℓ^1 method, and (3.3) implies

$$w^2(\mathcal{D}(\|\cdot\|_1, \mathbf{x})) \leq \Phi(s_r, s_g) = n - \frac{2}{\pi} \frac{(n - s_r)^2}{n}. \quad (3.4)$$

This bound is also meaningful, in view of the order sharp one, i.e. $\Phi_{\ell^1} = 2s_r \log(n/s_r) + 2s_r$ [52]. More precisely, (3.4) always represents a sharper upper bound than that in [52] for a signal with length $n = 10^5$ when the sparsity level $s_r < 5000$. Since conic Gaussian width is a typical tool for deriving lower bound for successful recovery, (3.4) may provide a tighter sampling bound for the ℓ^1 method.

Remark 2. *We further examine how the parameters n , λ_1 , λ_2 influence the variation of $\Phi(s_r, s_g)$ with respect to the sparsity levels s_r and s_g . Since $\Phi(\cdot, \cdot)$ only depends on the ratio of λ_1 and λ_2 , we may fix $\lambda_2 = 1$. For multiple combinations of n and λ_1 , since $s_g \leq 2s_r$ is always satisfied, we plot the function values of $\Phi(s_r, s_g)$ in the region $\{(s_r, s_g) | s_g \leq 2s_r\}$ in Fig. 2. The following observations can be drawn from the plots: (1) $\Phi(s_r, s_g)$ exhibits consistent patterns across different choices of n and λ_1 ; (2) $\Phi(s_r, s_g)$ is not sensitive to s_r , and remains relatively stable for fixed s_g , indicating that $\Phi(s_r, s_g)$ can dynamically reflect the influence of sparsity and gradient sparsity levels for estimating conic Gaussian width to some extent; (3) For fixed s_g , $\Phi(s_r, s_g)$ shows a monotonic increase pattern with respect to s_r , which may still make sense for certain small s_r according to Remark 1.*

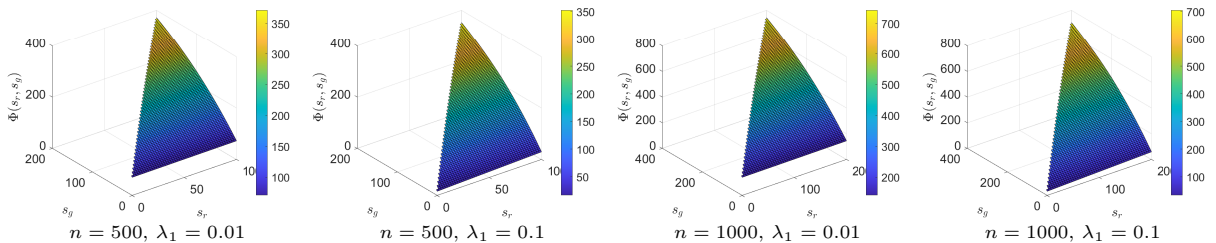


Figure 2: For fixed $\lambda_2 = 1$, plots of $\Phi(s_r, s_g)$ ($s_g \leq 2s_r$) under multiple settings of n and λ_1 .

Remark 3. *Let n_0 be an upper bound on the conic Gaussian width of the ℓ^1 or TV methods. We examine the case $\Phi(s_r, s_g) \leq n_0$ more closely. Direct computation shows*

$$2(n - s_r)^2 \left(\frac{\lambda_1}{\lambda_2} \right)^2 + b \frac{\lambda_1}{\lambda_2} + c \geq 0, \quad (3.5)$$

with $b = 4\sqrt{2}(n - s_r)(n - 1 - s_g) + (3n + 12 \min\{s_r, s_g\})n_0$ and $c = 4(n - 1 - s_g)^2 + 4(2n + s_g - 4)n_0$. (3.5) is a quadratic inequality in λ_1/λ_2 , whose solution in $\lambda_1/\lambda_2 > 0$ is always nonempty. That is, a proper choice of

Table 1: Comparisons of the upper bounds of conic Gaussian width for ℓ^1 , TV and ℓ^1 -TV methods with $n = 1000$.

Methods	$s_r = 50$		$s_r = 100$		$s_r = 150$	
	$s_g = 25$	$s_g = 50$	$s_g = 50$	$s_g = 100$	$s_g = 75$	$s_g = 150$
	$\lambda_1/\lambda_2 = 1$					
Φ_{ℓ^1} [52]	400	400	661	661	870	870
Φ_{TV} [17]	552	580	580	632	670	680
$\Phi(s_r, s_g)$	92	149	186	285	271	400
	$\lambda_1/\lambda_2 = 0.1$					
Φ_{ℓ^1} [52]	400	400	660	661	870	870
Φ_{TV} [17]	552	580	580	632	607	680
$\Phi(s_r, s_g)$	508	553	556	632	599	697

n , s_r , s_g and λ_2/λ_1 can always lead to a solution of (3.5). To shed insights, we compare $\Phi(s_r, s_g)$ with Φ_{ℓ^1} for ℓ^1 method (1.2) and Φ_{TV} for TV method (1.3) in Table 1. The table indicates that when $\lambda_1/\lambda_2 = 1$, $\Phi(s_r, s_g)$ can be much smaller than Φ_{ℓ^1} and Φ_{TV} , and in the relatively extreme case $\lambda_1/\lambda_2 = 0.1$ (i.e., gradient sparsity is dominating), the presence of sparsity can generally still improve $\Phi(s_r, s_g)$ over Φ_{TV} .

Using Theorem 3.1, we can give a recovery guarantee of the ℓ^1 -TV method. See Section 6.2 for the proof.

Theorem 3.2. Let $\mathbf{x}^* \in \mathbb{R}^n$, $\epsilon \geq 0$, $\mathbf{A} \in \mathbb{R}^{m \times n}$ whose rows are independent random vectors drawn from the standard Gaussian distribution $\mathcal{N}(\mathbf{0}, \mathbf{I}_n)$, and let $\mathbf{y} = \mathbf{A}\mathbf{x}^* + \mathbf{e} \in \mathbb{R}^m$ be the measurements. Suppose that $\|\mathbf{e}\|_2 \leq \epsilon$ and $\hat{\mathbf{x}}$ is the solution of the ℓ^1 -TV method (1.4). For certain $t > 0$, if

$$m > (\sqrt{\Phi(s_r, s_g)} + t)^2 + 1, \quad (3.6)$$

where $\Phi(s_r, s_g)$ is defined in (3.2) with $s_r(\mathbf{x})$ and $s_g(\mathbf{x})$ replaced by $s_r(\mathbf{x}^*)$ and $s_g(\mathbf{x}^*)$, then, with a probability at least $1 - e^{-\frac{t^2}{2}}$, there holds

$$\|\mathbf{x}^* - \hat{\mathbf{x}}\|_2 \leq \frac{2\epsilon}{\sqrt{m-1} - \Phi(s_r, s_g) - t}.$$

Remark 4. Theorem 3.2 gives robust recovery guarantee of the model (1.4). The sampling number for successful recovery depends on the regular sparsity level s_r and gradient sparsity level s_g of the signal \mathbf{x}^* to be recovered. By Remark 1, we can also obtain the sampling numbers of the ℓ^1 method and the TV method. If $\lambda_1 = 0$, the sampling number of the TV method defined by (3.6) is consistent with that from [17]. If $\lambda_2 = 0$, the sampling number for the robust recovery of the ℓ^1 method defined by (3.6) is $m > (\sqrt{n - \frac{2(n-s_r)^2}{n}} + t)^2 + 1$, which is sharper than $m > (\sqrt{2s_r \log(n/s_r)} + 2s_r + t)^2 + 1$ in [52] for certain n and s_r . Moreover, Remark 3 indicates that the sample complexity of the ℓ^1 -TV method can be better than both ℓ^1 [52] and TV [17] for suitable regimes for λ_1/λ_2 , s_r and s_g .

Remark 5. Note that we can simplify $\lambda_1\|\mathbf{x}\|_1 + \lambda_2\|\mathbf{D}\mathbf{x}\|_1$ as $\|\Psi\mathbf{x}\|_1$, where $\Psi = [\lambda_1\mathbf{I}_n; \lambda_2\mathbf{D}] \in \mathbb{R}^{(2n-1) \times n}$ is a frame with frame bounds λ_1 and $\sqrt{\lambda_1^2 + 4\lambda_2^2}$. The studies [10, 32, 33] have considered the case of Ψ being a general frame. Candès et al. [10] studied the case based on D-RIP (RIP adapted to Ψ), which is NP-hard to be verified. Kabanava et al. [32, 33] studied the construction of recovery condition via tangent cones. Genzel et al. [24] derived an explicit formula that describes the precise required number of measurements, whose bound depends on the coherence structure of Ψ . However, all of these studies do not treat the influence of the sparsity and gradient sparsity levels of the signal on the sampling number needed for robust recovery.

4 Fast learned solver for regularized ℓ^1 -TV model

The model (1.5) is numerically challenging due to its nonsmoothness and nonseparability. Existing algorithms, e.g., LADMM and S-FISTA, have shortcomings, e.g., dependence on additional hyper-parameters. Moreover, the iterative approach often suffers from relatively high cost. To mitigate these issues, we propose a novel algorithm and study its convergence, and then construct a fast learned solver by unrolling the proposed algorithm. Throughout, we also rewrite the model (1.5) as

$$\min_{\mathbf{x} \in \mathbb{R}^n} F(\mathbf{x}) = f(\mathbf{x}) + g(\mathbf{x}), \quad (4.1)$$

with $f(\mathbf{x}) = \frac{1}{2}\|\mathbf{y} - \mathbf{A}\mathbf{x}\|_2^2$, $g(\mathbf{x}) = g_1(\mathbf{x}) + g_2(\mathbf{x})$ with $g_1(\mathbf{x}) = \lambda_1\|\mathbf{x}\|_1$ and $g_2(\mathbf{x}) = \lambda_2\|\mathbf{x}\|_{\text{TV}}$.

¹For any $\mathbf{x} \in \mathbb{R}^n$, the inequalities $\lambda_1\|\mathbf{x}\|_2 \leq \|\Psi\mathbf{x}\|_2 \leq \sqrt{\lambda_1^2 + 4\lambda_2^2}\|\mathbf{x}\|_2$ can be easily checked by using the estimate $\|\mathbf{D}\|_2 \leq 2$ [64, Lemma 8.11].

4.1 Proximal gradient mapping method

First we construct a proximal gradient mapping method, prove its global convergence and discuss the parameter selection criterion.

4.1.1 Construction of proximal gradient mapping method

We first recall the proximal gradient descent method and gradient mapping operator, which are crucial for constructing the proximal gradient mapping method. The goal of the proximal gradient descent method [5] is to find a minimum of the function $f + g$, where f is convex and smooth (with a Lipschitz constant L_f), and g is convex, not necessarily smooth. It consists of the following iterative step

$$\mathbf{x}^{k+1} = \text{prox}_{\frac{1}{L_f}g} \left(\mathbf{x}^k - \frac{1}{L_f} \nabla f(\mathbf{x}^k) \right). \quad (4.2)$$

When $g(\mathbf{x}) = \|\mathbf{x}\|_1$, the iterative step (4.2) has a closed form solution (see (2.7)), resulting in ISTA or FISTA. However, this family of methods cannot be directly employed to solve (1.5) with $g(\mathbf{x}) = \lambda_1 \|\mathbf{x}\|_1 + \lambda_2 \|\mathbf{x}\|_{\text{TV}}$. In fact, since $g(\cdot)$ is a sum of ℓ^1 composite terms, computing $\text{prox}_g(\cdot)$ is no longer separable and ISTA loses its effectiveness. In addition, the gradient mapping operator of f and g is given by

$$\mathcal{G}_{L_f}^{f,g}(\mathbf{x}) = L_f \left(\mathbf{x} - \text{prox}_{\frac{1}{L_f}g} \left(\mathbf{x} - \frac{1}{L_f} \nabla f(\mathbf{x}) \right) \right).$$

Then the ISTA update step in (4.2) can be rewritten as $\mathbf{x}^{k+1} = \mathbf{x}^k - \frac{1}{L_f} \mathcal{G}_{L_f}^{f,g}(\mathbf{x}^k)$, which takes the form of a gradient descent step. $\mathcal{G}_{L_f}^{f,g}(\cdot)$ generalizes the gradient of $f(\mathbf{x})$:

$$\begin{cases} \mathcal{G}_{L_f}^{f,g}(\mathbf{x}) = \nabla h(\mathbf{x}) = \nabla f(\mathbf{x}), & \text{if } g(\mathbf{x}) \equiv 0, \\ \mathcal{G}_{L_f}^{f,g}(\mathbf{x}^*) = 0, & \text{if and only if } \mathbf{x}^* \text{ is a minimizer of } f + g. \end{cases}$$

See [5] for more details about the gradient mapping operator.

Now we can develop a proximal gradient mapping (PGM) method. For problem (1.5), motivated by the proximal gradient descent method and gradient mapping operator, we propose to solve (4.1) using a PGM method, which takes an update of the form

$$\mathbf{x}^{k+1} = \text{prox}_{tg_2} \left(\mathbf{x}^k - t \mathcal{G}_{1/u}^{f,g_1}(\mathbf{x}^k) \right),$$

where $u > 0$ and $t > 0$ are constants to be specified. This update involves computing $\text{prox}_{ug_1}(\cdot) = \mathcal{S}_{\lambda_1 u}(\mathbf{x})$ and $\text{prox}_{tg_2}(\cdot) = \mathcal{T}_{\lambda_2 t}(\mathbf{x})$ (see (4.1) for $g_1(\cdot)$ and $g_2(\cdot)$), both of which can be carried out efficiently. Thus, the proposed PGM method with the inner update step being the soft threshold shrinkage and the outer update step being the proximal TV (PGM-ISTA for short) can be concisely written as

$$\mathbf{x}^{k+1} = \mathcal{T}_{\lambda_2 t} \left(\left(1 - \frac{t}{u} \right) \mathbf{x}^k + \frac{t}{u} \mathcal{S}_{\lambda_1 u}(\mathbf{x}^k - u \mathbf{A}^\top (\mathbf{A} \mathbf{x}^k - \mathbf{y})) \right).$$

The whole procedure of PGM-ISTA is given in Algorithm 1. PGM-ISTA involves two adjustable parameters (i.e., u and t) due to the two parameters in the ℓ^1 -TV objective.

Algorithm 1 PGM-ISTA

Input: $(f, g_1, g_2, \mathbf{x}^0)$, where f, g_1 and g_2 satisfy (4.1), and $\mathbf{x}^0 \in \mathbb{R}^n$.

Initialization: pick $u > 0, t > 0$.

General Step: for $k = 0, 1, 2, \dots$, excute the following steps:

(a) set $\mathcal{G}_{1/u}^{f,g_1}(\mathbf{x}^k) = \frac{1}{u} (\mathbf{x}^k - \text{prox}_{ug_1}(\mathbf{x}^k - u \nabla f(\mathbf{x}^k)))$;

(b) set $\mathbf{x}^{k+1} = \text{prox}_{tg_2}(\mathbf{x}^k - t \mathcal{G}_{1/u}^{f,g_1}(\mathbf{x}^k))$.

4.1.2 Global convergence and parameter selection criterion for PGM-ISTA

It is natural to ask whether PGM-ISTA converges to the optimal solution of (1.5). Now we discuss its global convergence and parameter selection criterion. The proof of the next result is given in Section 6.3.

Theorem 4.1. *Let $\{\mathbf{x}^k(u, t)\}_{k \geq 0}$ be a sequence generated by Algorithm 1. Then the following statements hold.*

(a) *There exist $u > 0$ and $t > 0$ such that $\{\mathbf{x}^k(u, t)\}_{k \geq 0}$ converges to the optimal solution of problem (1.5);*

(b) Suppose $u \in (0, 2/\|\mathbf{A}\|_2^2)$, $t \in (0, u]$. Then, $\{\mathbf{x}^k(u, t)\}_{k \geq 0}$ converges to a fixed point $\mathbf{x}(u, t)$:

$$\mathbf{x}(u, t) = \text{prox}_{t g_2} \left(\mathbf{x}(u, t) - t \mathcal{G}_{1/u}^{f, g_1}(\mathbf{x}(u, t)) \right). \quad (4.3)$$

Remark 6. The proof of Theorem 4.1 (a) indicates that if the parameter pair (u_0, t_0) provides a convergent sequence generated by Algorithm 1, smaller parameter pair (u, t) with $u \leq u_0$ and some $t > 0$ also generates a convergent sequence.

Remark 7. Theorem 4.1(b) indicates that for $u \in (0, 2/\|\mathbf{A}\|_2^2)$ and $t \in (0, u]$, the sequence generated by Algorithm 1 always converges to some fixed point \mathbf{x}^∞ , that is

$$\mathbf{x}^\infty = \text{prox}_{t g_2} \left(\left(1 - \frac{t}{u}\right) \mathbf{x}^\infty + \frac{t}{u} \hat{\mathbf{x}} \right), \quad (4.4)$$

with $\hat{\mathbf{x}} = \text{prox}_{u g_1}(\mathbf{x}^\infty - u \nabla f(\mathbf{x}^\infty))$. Therefore, by [5, Theorem 6.39], (4.4) holds if and only if

$$\exists \mathbf{w}_1 \in \partial g_1(\hat{\mathbf{x}}), \mathbf{w}_2 \in \partial g_2(\mathbf{x}^\infty) \quad \text{s.t.} \quad \mathbf{w}_1 + \mathbf{w}_2 + \nabla f(\mathbf{x}^\infty) = \mathbf{0}.$$

By Fermat's optimality condition [5, Theorem 3.63], $\mathbf{x}^* \in \mathbb{S}^*$ is an optimal solution of (4.1) if and only if

$$\exists \mathbf{w}_1 \in \partial g_1(\mathbf{x}^*), \mathbf{w}_2 \in \partial g_2(\mathbf{x}^*) \quad \text{s.t.} \quad \mathbf{w}_1 + \mathbf{w}_2 + \nabla f(\mathbf{x}^*) = \mathbf{0}.$$

These two observations imply that a sufficient condition for the fixed point \mathbf{x}^∞ to be the optimal solution of (1.5) is $\hat{\mathbf{x}} = \mathbf{x}^\infty$. These discussions indicate that \mathbf{x}^∞ may not be the optimal solution of (4.1).

Now we discuss the parameter selection strategy. Theorem 4.1 not only shows that there always **exists** a parameter pair (u, t) for Algorithm 1 to generate a convergent sequence to the optimal solution of (4.1), but also provides guidelines for choosing the parameter pair (u, t) . Remark 7 indicates that although a fixed point of Algorithm 1 may not necessarily be an optimal solution of (4.1), it narrows down the feasible range since the optimal solution must be a fixed point. Naturally, if we define the set of fixed points of Algorithm 1 by

$$\mathbb{F} = \left\{ \mathbf{x}(u, t) \in \mathbb{R}^n \mid u \in \left(0, \frac{2}{\|\mathbf{A}\|_2^2}\right), t \in (0, u] \right\}, \quad (4.5)$$

then Theorem 4.1 implies $\mathbb{S}^* \cap \mathbb{F} \neq \emptyset$ (empty set).

The next theorem further investigates the influence of the parameter pair (u, t) on the convergence of Algorithm 1, provided that $g_1(\cdot)$ has a bounded domain $\text{dom}(g_1) \subset \{\mathbf{x} : \|\mathbf{x}\|_2 \leq r\}$ for sufficiently large r . Thus, for any $\mathbf{x} \in \text{dom}(g_1)$, the gradient ∇f of f can be bounded by

$$\|\nabla f(\mathbf{x})\|_2 \leq r \|\mathbf{A}\|_2^2 + \|\mathbf{A}^\top \mathbf{y}\|_2. \quad (4.6)$$

The proof is deferred to Section 6.4.

Theorem 4.2. Let $u \in (0, 2/\|\mathbf{A}\|_2^2)$, $t \in (0, 3u/4)$. Then for any $\epsilon > 0$, if $k \in \mathbb{N}$ is sufficiently large such that

$$\|\mathbf{x}^k - \mathbf{x}^{k+1}\|_2 \leq t\epsilon, \quad (4.7)$$

we have

$$F(\mathbf{x}^{k+1}) - F(\mathbf{x}^*) \leq 2r\epsilon + (t\kappa + \beta)u,$$

with $\mathbf{x}^* = \arg \min_{\mathbf{x}} F(\mathbf{x})$ and

$$\begin{aligned} \kappa &= \left(\|\mathbf{A}\|_2^2 r + \|\mathbf{A}^\top \mathbf{y}\|_2 + \lambda_2 \|\mathbf{D}\|_2 + \lambda_1 \right) \|\mathbf{A}\|_2^2 (\|\mathbf{A}\|_2^2 r + \|\mathbf{A}^\top \mathbf{y}\|_2 + \lambda_1), \\ \beta &= 2r \|\mathbf{A}\|_2^2 (\|\mathbf{A}\|_2^2 r + \|\mathbf{A}^\top \mathbf{y}\|_2 + \lambda_1) + (\|\mathbf{A}\|_2^2 r + \|\mathbf{A}^\top \mathbf{y}\|_2) (\|\mathbf{A}\|_2^2 r + \lambda_1) + \frac{\lambda_1^2}{2}. \end{aligned}$$

Remark 8. Theorem 4.2 shows that for $u \in (0, 2/\|\mathbf{A}\|_2^2)$ and $t \in (0, 3u/4)$, the error in the function value is controlled by $2r\epsilon + (t\kappa + \beta)u$, and thus a smaller u will lead to smaller errors in the function value for any fixed ϵ . This and Theorem 4.1 show that we need smaller u and proper t to get a smaller objective function error in practice, i.e., a balance between u and t in order to achieve a better rate of convergence.

4.2 Construction of fast learned solver

In this part, we construct a learned solver for the model (1.5) by unrolling PGM-ISTA. The discussions in Section 4.1 suggest that the PGM-ISTA scheme can provide an efficient iterative solver for the model (1.5). By setting the first iteration of PGM-ISTA to $\mathbf{x}^0 = \mathbf{0}$, it becomes

$$\mathbf{x}^1 = \mathcal{T}_{t\lambda_2}(\frac{t}{u}\mathcal{S}_{u\lambda_1}(u\mathbf{A}^\top \mathbf{y})). \quad (4.8)$$

Formally this can be viewed as a neural network with two layers. Next, we present more evidences to elucidate the point. Indeed, by setting proper learnable parameters, the ISTA with the soft threshold operator \mathcal{S}_λ can be extended to a recurrent network, i.e., learned ISTA (LISTA) [26]. Thus, the inner part of (4.8) (i.e., $\mathcal{S}_{u\lambda_1}(\cdot)$) can be regarded as one layer of a neural network similar to LISTA. Further, the study on the TV proximal operator [14] shows that the outer part of (4.8) (i.e. $\mathcal{T}_{t\lambda_2}(\cdot)$) can also be learned. These useful findings are summarized in the following proposition.

Proposition 4.1 ([14, Weak Jacobian of prox-TV]). *Let $\mathbf{x} \in \mathbb{R}^n$ and $\mathbf{z} = \mathcal{T}_\mu(\mathbf{x})$, and \mathbb{S} be the support of $\tilde{\mathbf{D}}\mathbf{z}$ with $\tilde{\mathbf{D}} = [[1, 0, \dots, 0]; \mathbf{D}]$. Then, the weak Jacobian $J_{\mathbf{x}}$ and J_μ of $\mathcal{T}_\mu(\mathbf{x})$ with respect to \mathbf{x} and μ are given by*

$$\begin{cases} J_{\mathbf{x}}(\mathbf{x}, \mu) = \mathbf{L}_{:, \mathbb{S}}(\mathbf{L}_{:, \mathbb{S}}^\top \mathbf{L}_{:, \mathbb{S}})^{-1} \mathbf{L}_{:, \mathbb{S}}^\top, \\ J_\mu(\mathbf{x}, \mu) = -\mathbf{L}_{:, \mathbb{S}}(\mathbf{L}_{:, \mathbb{S}}^\top \mathbf{L}_{:, \mathbb{S}})^{-1} \text{sign}(\mathbf{D}\mathbf{z})_{\mathbb{S}}, \end{cases} \quad \text{with } \mathbf{L} = \begin{bmatrix} 1 & 0 & \cdots & 0 \\ 1 & 1 & \cdots & 0 \\ \vdots & \vdots & \ddots & \vdots \\ 1 & 1 & \cdots & 1 \end{bmatrix} \in \mathbb{R}^{n \times n}.$$

Proposition 4.1 gives the weak Jacobians of $\mathcal{T}_\mu(\mathbf{x})$ respect to \mathbf{x} and μ , which can be employed via back-propagation. Moreover, the dependency in the inputs is only through \mathbb{S} and $\text{sign}(\mathbf{D}\mathbf{z})$. Hence, computing these weak Jacobians can be done efficiently by simply storing $\text{sign}(\mathbf{D}\mathbf{z})$ as a mask, as it would be done for a ReLU or the soft-thresholding activation functions, and requiring just $2(n-1)$ bits.

Now one may interpret some neural networks as approximate algorithms for solving (1.5). To this end, let $\mathbf{W}_y = u\mathbf{A}^\top$, $\mathbf{W}_x = \mathbf{I}_n - u\mathbf{A}^\top \mathbf{A}$. Then, a general iteration of PGM-ISTA takes the form

$$\mathbf{x}^{k+1} = \mathcal{T}_{\lambda_2 t} \left((1 - \frac{t}{u}) \mathbf{x}^k + \frac{t}{u} \mathcal{S}_{\lambda_1 u} (\mathbf{W}_x \mathbf{x}^k + \mathbf{W}_y \mathbf{y}) \right). \quad (4.9)$$

Fig. 3 (a) depicts PGM-ISTA for problem (1.5), and the theoretical findings in Section 4.1.2 ensure the convergence of iteration (4.9) with properly chosen $u \in (0, 2/\|\mathbf{A}\|_2^2)$ and $t \in (0, u]$. By unrolling the architecture with L layers, we obtain a network $\text{net}(\mathbf{y}; \Theta^L) = \mathbf{x}^L$ which is termed as learned PGM-ISTA (LPGM-ISTA) with learnable parameters $\Theta^L = \{\mathbf{W}_x, \mathbf{W}_y, u, t\}$, cf. Fig. 3 (b) for a schematic illustration.

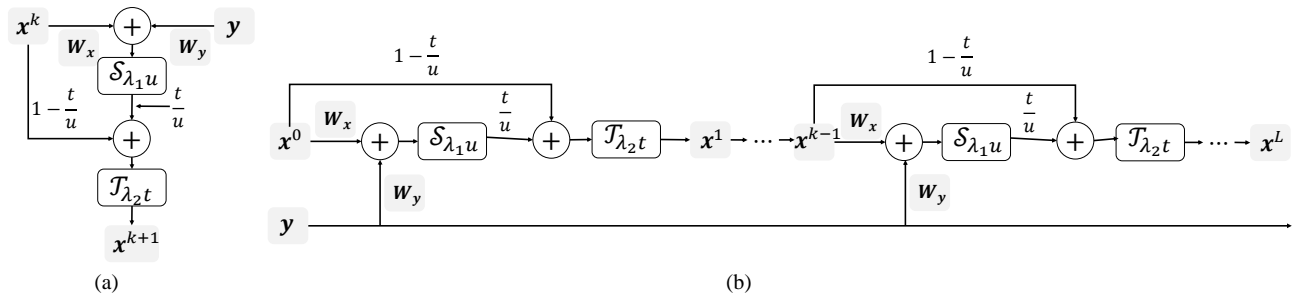


Figure 3: Neural network representation of PGM-ISTA. (a) PGM-ISTA; (b) LPGM-ISTA obtained by unfolding PGM-ISTA with L layers, and the learnable parameters are $\Theta^L = \{\mathbf{W}_x, \mathbf{W}_y, u, t\}$.

By Remark 8, a good choice of u and t is crucial in order to achieve fast convergence. In practice, the parameter selection scheme from the theory of PGM-ISTA can be used to initialize the training stage. The goal of the learning process is to find the parameter vector Θ^L that minimizes the loss or the expected loss over a suitable training data distribution, which is however unavailable. The empirical risk minimization framework with a given training set $\{(\mathbf{y}_i, \mathbf{x}_i)\}_{i=1}^N$ is a practical choice. Thus, the neural network is trained by minimizing the following loss function

$$\min_{\Theta^L} \frac{1}{N} \sum_{i=1}^N \|\mathbf{x}_i - \text{net}(\mathbf{y}_i; \Theta^L)\|_2^2. \quad (4.10)$$

Note that when $k \rightarrow +\infty$, proper initialization in (4.9) gives a global solution of the loss for all \mathbf{y}_i , and the network thus converges to the exact minimum of (1.5). However, when $k = L$ is fixed, or the initialization parameters are not chosen properly, the output of the network is generally not a solution of (1.5). Therefore,

minimizing the empirical risk is actually to identify a parameter configuration that effectively alleviates the sub-optimality of the network with respect to (1.5) across the input distribution utilized for training. In this way, the network is trained to acquire an algorithm that can effectively approximate the solution of (1.5) for a specific category of signal distributions. Note that although the procedure can effectively expedite the resolution of the problem, the learned algorithm will only be effective for inputs \mathbf{y}_i within the same input distribution as the training samples (i.e., in-distribution test). It may fail to deliver accurate approximations for samples that deviate significantly from the training set (i.e., out-of-distribution), in contrast to the iterative algorithm itself, which is guaranteed to converge regardless of the sample.

In addition, the selection of penalty parameters holds great importance. Indeed, if λ_1 and λ_2 are big enough such that $\lambda_1 + 2\lambda_2 \geq \lambda_{\max}$ (see Lemma 4.1 below), then the model (1.5) has only $\mathbf{0}$ as its solution. Therefore, it is crucial to select suitable penalty parameters for the model (1.5). Fortunately, unrolled networks naturally inherit prior structures and domain knowledge rather than learn this information from intensive training data [43], and we can initialize the penalty parameter pair (λ_1, λ_2) based on the algorithm itself.

Lemma 4.1. *Denote λ_{\max} as the smallest value of the penalty parameter such that $\mathbf{0}$ is a solution. The value λ_{\max} of the model (1.5) is $\lambda_{\max} = \|\mathbf{A}^\top \mathbf{y}\|_\infty$.*

Proof. The first order conditions for problem (1.5) reads: for $\mathbf{0} \in \mathbb{R}^n$

$$\mathbf{0} \in \partial F(\mathbf{0}) = \mathbf{A}^\top \mathbf{y} + \lambda_1 \partial \|\cdot\|_1(\mathbf{0}) + \lambda_2 \mathbf{D}^\top \|\cdot\|_1(\mathbf{D}\mathbf{0}).$$

Upon expanding the equality, we have

$$\mathbf{a}_j^\top \mathbf{y} \in \begin{cases} [-(\lambda_1 + \lambda_2), (\lambda_1 + \lambda_2)], & j = 1, \\ [-(\lambda_1 + 2\lambda_2), (\lambda_1 + 2\lambda_2)], & j \in \{2, 3, \dots, n\}. \end{cases}$$

Thus, $\mathbf{0}$ is a solution of the model (1.5) for all $\lambda_1 + 2\lambda_2 \geq \lambda_{\max}$, with $\lambda_{\max} = \|\mathbf{A}^\top \mathbf{y}\|_\infty$. \square

Note that LPGM-ISTA is designed to efficiently solve the regularized model (1.5) with fixed λ_1 and λ_2 , by unrolling PGM-ISTA for a fixed number of iterations. It is interesting to learn the parameters λ_1 and λ_2 simultaneously. For example, Scetbon et al [48] proposed a multi-layer perceptron (MLP) network for learning regularization parameters in the K-SVD algorithm. This idea may be useful for learning the parameters λ_1 and λ_2 in PGM-ISTA. We plan to explore the issue in future works.

5 Numerical experiments and discussions

In this section, we carry out some numerical experiments on the sampling number obtained in Section 3 and the influence of parameters (u, t) in PGM-ISTA, and the application of LPGM-ISTA to recover ECG signals. All the experiments are conducted on a desktop with Intel Core i9-13900K processor (3.00GHz, 64GB RAM) and NVIDIA GeForce RTX 4080 (16GB RAM).

5.1 Synthetic experiments for sampling number

In this part, we conduct synthetic experiments for the sampling number in Section 3, including a comparison with previous works. We shall consider $\epsilon = 0$, and study the bound (3.6) for the sampling number in several situations. Then we can fix $\lambda_2 = 1$ such that there is only λ_1 to be tuned. Note that PGM-ISTA is designed for the regularized ℓ^1 -TV method (1.5) with $\epsilon \geq 0$, which involve two penalty parameters λ_1 and λ_2 . Moreover, since the constrained model (1.4) with $\epsilon = 0$ involves only one parameter and can be solved exactly by alternating direction method of multipliers (ADMM), we implement the model (1.4) by ADMM instead of PGM-ISTA in this part.

To develop the ADMM for the model (1.4), we rewrite as

$$\min_{\mathbf{x} \in \mathbb{R}^n} g(\mathbf{x}), \quad \text{s.t.} \quad \mathbf{y} = \mathbf{A}\mathbf{x}. \quad (5.1)$$

Let $\mathbf{x} = \mathbf{z}$, where \mathbf{z} is an auxiliary variable. Then we obtain

$$\min_{\mathbf{x}, \mathbf{z} \in \mathbb{R}^n} g(\mathbf{z}), \quad \text{s.t.} \quad \begin{bmatrix} \mathbf{A} \\ \mathbf{I}_n \end{bmatrix} \mathbf{x} = \begin{bmatrix} \mathbf{y} \\ \mathbf{z} \end{bmatrix}. \quad (5.2)$$

The augmented Lagrangian function is given by

$$g(\mathbf{z}) + \mathbf{u}^\top (\mathbf{A}\mathbf{x} - \mathbf{y}) + \frac{\mu}{2} \|\mathbf{A}\mathbf{x} - \mathbf{y}\|_2^2 + \mathbf{v}^\top (\mathbf{x} - \mathbf{z}) + \frac{\mu}{2} \|\mathbf{x} - \mathbf{z}\|_2^2,$$

where \mathbf{u} and \mathbf{v} are dual variables. Following the procedure of ADMM, we update the variables alternately.

- For the term involving \mathbf{x}

$$\begin{aligned}\mathbf{x}^{k+1} &= \arg \min_{\mathbf{x}} \mathbf{u}^{k,\top} (\mathbf{A}\mathbf{x} - \mathbf{y}) + \frac{\mu^k}{2} \|\mathbf{A}\mathbf{x} - \mathbf{y}\|_2^2 + \mathbf{v}^{k,\top} (\mathbf{x} - \mathbf{z}^k) + \frac{\mu^k}{2} \|\mathbf{x} - \mathbf{z}^k\|_2^2 \\ &= (\mathbf{A}^\top \mathbf{A} + \mathbf{I})^{-1} (\mathbf{A}^\top \mathbf{y} + \mathbf{z}^k - \frac{1}{\mu^k} \mathbf{A}^\top \mathbf{u}^k - \frac{1}{\mu^k} \mathbf{v}^k).\end{aligned}\quad (5.3)$$

- For the term involving \mathbf{z} , by Lemma 2.2, we have

$$\mathbf{z} = \arg \min_{\mathbf{z}} g(\mathbf{z}) + \frac{\mu^k}{2} \|\mathbf{x}^{k+1} - \mathbf{z} + \frac{\mathbf{v}^k}{\mu^k}\|_2^2 = \mathcal{P}_{\lambda_1/\mu^k}^{\lambda_2/\mu^k} \left(\mathbf{x}^{k+1} + \frac{\mathbf{v}^k}{\mu^k} \right).\quad (5.4)$$

We summarize the whole update procedure in Algorithm 2. Since this is a two block ADMM, the global convergence is guaranteed [8].

Algorithm 2 ADMM for problem (5.2)

Input: Sensing matrix \mathbf{A} , measurement \mathbf{y} .

1: Initialization: $\mathbf{x}^0, \mathbf{z}^0$ being zero vectors, regularization parameters λ_1, λ_2 , tolerate error $tol = 10^{-8}$, $\mu^0 = 10^{-3}$, $\rho = 1.1$, $\mu_{max} = 10^8$, and $k = 0$.

while not convergent **do**

2: Update \mathbf{x}^{k+1} by (5.3);

3: Update \mathbf{z}^{k+1} by (5.4);

4: $\mathbf{u}^{k+1} = \mathbf{u}^k + \mu^k (\mathbf{A}\mathbf{x}^{k+1} - \mathbf{y})$;

5: $\mathbf{v}^{k+1} = \mathbf{v}^k + \mu (\mathbf{x}^{k+1} - \mathbf{z}^{k+1})$;

6: $\mu^{k+1} = \min\{\rho\mu^k, \mu_{max}\}$;

7: Check the convergence condition

$$\|\mathbf{x}^{k+1} - \mathbf{x}^k\|_2 / \max\{\|\mathbf{x}^k\|_2, 1\} < tol;$$

8: Update $k \leftarrow k + 1$;

9: **end while**

Output: $\hat{\mathbf{x}} = \mathbf{x}^{k+1}$.

Next, we carry out simulations to complement the theory in Section 3. Since the ℓ^1 -TV model enforces sparsity both in signal itself and the differences between consecutive components of the signal, we conduct experiments on signals that are locally constant and change in jumps, following the setting in [63]. Specifically, we generate the synthetic signal $\mathbf{x}^* \in \mathbb{R}^n$ in four steps: (i) Set $\|\mathbf{x}^*\|_0 = s_r < n$; (ii) To ensure the local-smooth property of \mathbf{x}^* , we generate b ($b \in \mathbb{N}$) blocks randomly with block size 10, and elements in each block have the same amplitude, sampled from the standard normal distribution $\mathcal{N}(0, 1)$; (iii) we generate $s_r - 10b$ locations with their amplitudes following $\mathcal{N}(0, 1)$; (iv) we normalize the signal \mathbf{x}^* to the interval $[-1, 1]$ by $\mathbf{x}^* / \max|\mathbf{x}^*|$. The Gaussian sampling strategy on \mathbf{A} stated in Theorem 3.2 is adopted. To illustrate the recovery accuracy, we show in Fig. 4 one synthetic signal with $n = 1000$, $s_r = 300$ and $b = 12$, and its recovered signal by ℓ^1 -TV method under $\epsilon = 0$ with a sampling ratio of 0.5.

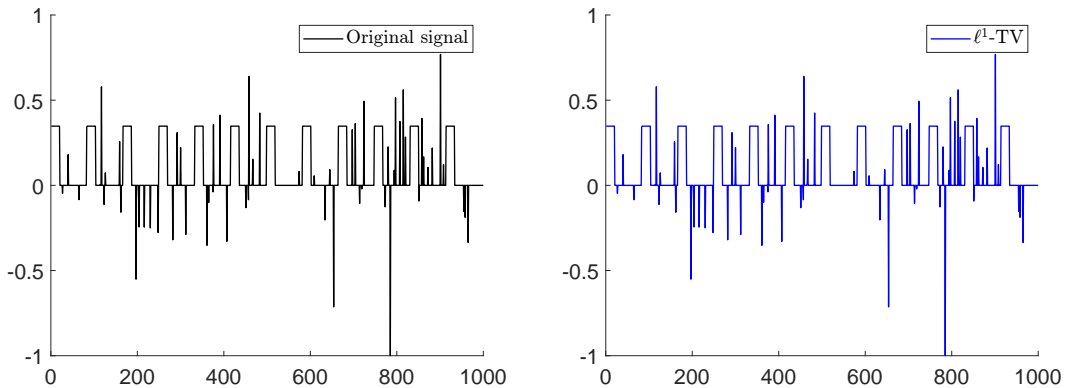


Figure 4: A synthetic signal and its recovered one by the ℓ^1 -TV method.

We first examine the influences of the parameters λ_1 and λ_2 on the recovery performance. We simply set $\lambda_2 = 1$ in the model (1.4), and thus we only test the influence of λ_1 . To this end, we choose λ_1 from the set $\{1, 10^{-1}, 10^{-2}, 10^{-3}, 10^{-4}, 10^{-5}\}$ by cross-validation. Moreover, we consider different n , s_r and s_g , and plot the relative errors versus λ_1 in Fig. 5. For a recovered signal $\hat{\mathbf{x}}$ with the clean signal \mathbf{x}^* , we define the relative error (RelErr) as $\text{RelErr}(\hat{\mathbf{x}}, \mathbf{x}^*) = \|\hat{\mathbf{x}} - \mathbf{x}^*\|_2 / \|\mathbf{x}^*\|_2$. It is observed that $\lambda_1 = 10^{-3}$ is a good choice in all cases.

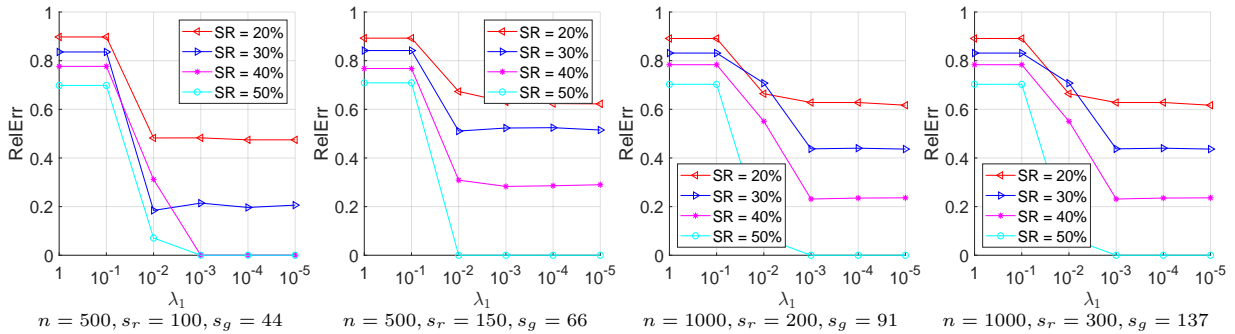


Figure 5: Selections of λ_1 for fixed $\lambda_2 = 1$ under different situations.

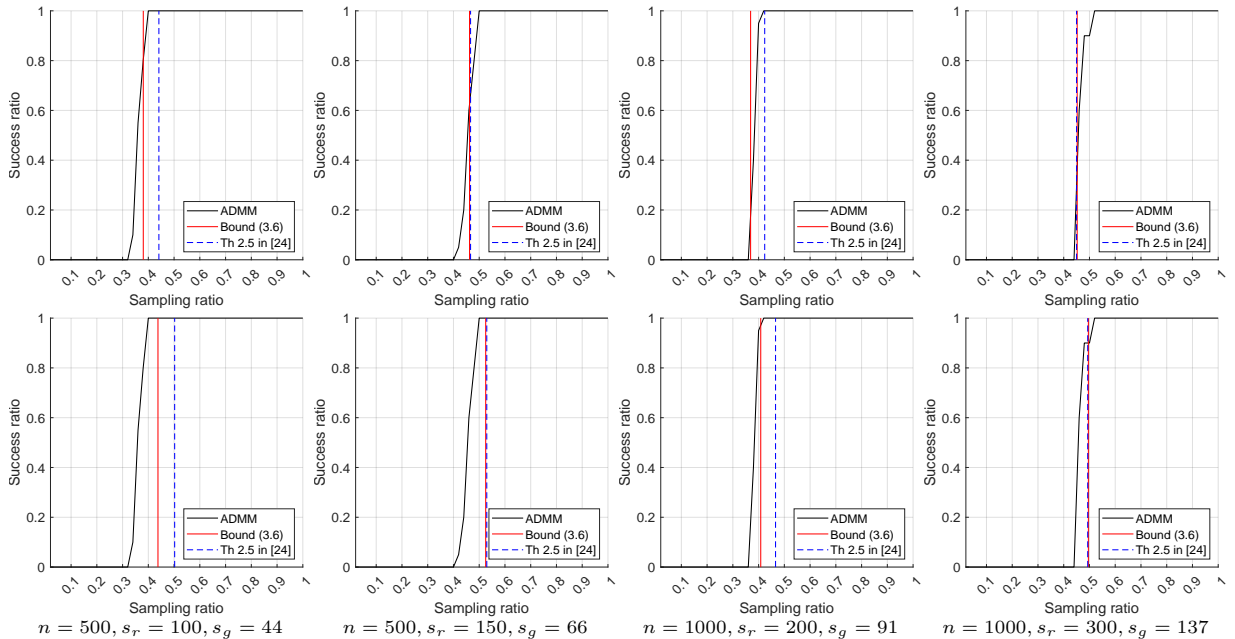


Figure 6: The theoretical bound (3.6) and the bound from Theorem 2.5 of [24] at different sparsity levels, with $t = 1$ (top row) and $t = 2$ (bottom row).

Further, for different signal lengths and sparsity levels, we examine the influence of the sampling number m on the recovery performance. To this end, for each sampling ratio m/n , we repeat the experiments 50 times and declare success for the recovered signal $\hat{\mathbf{x}}$ if $\|\mathbf{x}^* - \hat{\mathbf{x}}\|_2 < 10^{-3}$. The curves in Fig. 6 show the success ratio with respect to the sampling ratio, along with the bound (3.6) and the bound stated in Theorem 2.5 of [24], representing the required number of scaled form samples for successful recovery. Compared with the bound due to [24] under the condition of $t = 1$ (with a probability $1 - e^{-t^2/2} \approx 0.3935$) and $t = 2$ (with a probability $1 - e^{-t^2/2} \approx 0.8647$), the bound (3.6) can more faithfully estimate the sampling number m needed for successful recovery, which appears tighter in the simulations, especially for relatively low levels of regular sparsity and gradient sparsity.

5.2 Parameters influence for PGM-ISTA

Now we study the influence of the parameter pair (u, t) on the convergence of PGM-ISTA. We choose one ECG signal from the MIT-BIH Arrhythmia Database [44] as the signal to be recovered. The ECG signal is windowed to 1024 samples, cf. Fig. 1. The sensing matrix \mathbf{A} is Gaussian, and the measurements are contaminated by Gaussian noise with variance 0.01 and a sampling ratio 0.5.

The PGM-ISTA algorithm and its learned counterpart include one parameter pair (u, t) and the model (1.5) contains two penalty parameters λ_1 and λ_2 . The first experiment aims to verify the existence of a parameter pair (u, t) by cross-validation for fixed penalty parameters. We take $\lambda_1 = \lambda_2 = 0.01$, and conduct an experiment with both u and t being in an increasing order and equi-spaced for $u \in (0, 2/\|\mathbf{A}\|_2^2)$ and $t \in (0, u]$ by Theorem 4.1, respectively. For each pair (u, t) , we set the maximum number of iterations to 1000, and the results are shown in Fig. 7. Fig. 7 (a) shows that there are many pairs (u, t) for which PGM-ISTA achieves the goal $F(\mathbf{x}^k) - F(\mathbf{x}^*) < 0.01$ within 1000 iterations. Thus, there is a large region of (u, t) providing convergent sequences for both PGM-ISTA if we declare convergence under the criterion $F(\mathbf{x}^k) - F(\mathbf{x}^*) < 0.01$ for some

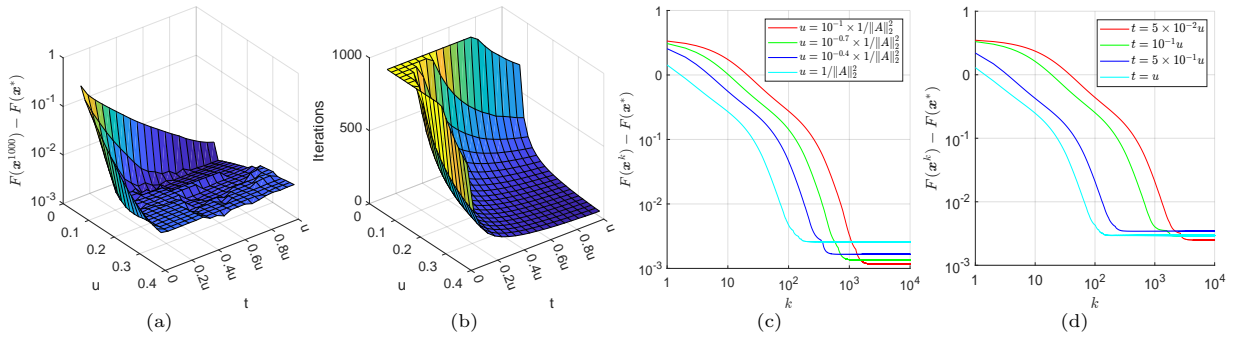


Figure 7: The convergence of PGM-ISTA for fixed $\lambda_1 = \lambda_2 = 0.01$, (a) shows values of $F(\mathbf{x}^{1000}(u, t)) - F(\mathbf{x}^*)$; (b) shows the minimum iteration k such that $F(\mathbf{x}^k(u, t)) - F(\mathbf{x}^*) < 0.01$; (c) shows values of $F(\mathbf{x}^k(u, t)) - F(\mathbf{x}^*)$ with multiple choices of u and $t = 0.9u$; (d) shows values of $F(\mathbf{x}^k(u, t)) - F(\mathbf{x}^*)$ for multiple choices of t and $u = 1/\|\mathbf{A}\|_2^2$.

$k \in \mathbb{N}_+$. Fig. 7 (b) shows the number of PGM-ISTA iterations needed to achieve $F(\mathbf{x}^k) - F(\mathbf{x}^*) < 0.01$. Clearly, bigger values of pair (u, t) may result in faster convergence. The numerical results contrast slightly the theoretical prediction of Theorem 4.2 which suggests that a smaller u may give a smaller error in the function value for PGM-ISTA. This is attributed to the fact that we only run PGM-ISTA for a maximum of 1000 iterations, which seems not enough occasionally. Further experiments indicate that a small u may lead to slower convergence. Hence, we have increased the number of iterations for several choices of u , and the results are shown in Fig. 7 (c). Then indeed a smaller u leads to a smaller function error, which agrees well with the theoretical results from Theorem 4.2, but a smaller u does require more iterations to reach the desired convergence.

Next, we explore how the parameter t affects the convergence rate in terms of the function value. We conduct an experiment for fixed $u = 1/\|\mathbf{A}\|_2^2$ and different t , and Fig. 7 (d) shows the results. Obviously, the influence of t about the function value is slight, but indeed a bigger t may lead to faster convergence.

Finally, we compare the performance of the ℓ^1 , TV and ℓ^1 -TV methods when the observation data are contaminated by additive i.i.d. Gaussian noise (with a standard deviation σ). We choose σ from the set $\{0, 0.01, 0.1\}$ and the signal in Fig. 4 as the ground truth, and summarize the relative errors of the recovered signals by the three methods in Table 2. It is observed that ℓ^1 -TV can obtain much smaller relative errors in all cases, showing its superiority when the exact signal exhibits both signal sparsity and gradient sparsity. Also we plot the exact signal and the recovered ones with $\sigma = 0$ in Fig. 8, which again confirms that ℓ^1 -TV performs better than the ℓ^1 or TV methods. Note that the algorithm ADMM cannot be used when $\sigma \neq 0$.

Table 2: Relative errors of three methods under $\sigma \in \{0, 0.01, 0.1\}$.

Methods	$\sigma = 0$	$\sigma = 0.01$	$\sigma = 0.1$
ℓ^1	0.7000	0.7488	0.7516
TV	0.1025	0.1224	0.1296
ℓ^1 -TV	0.0027	0.0088	0.0793

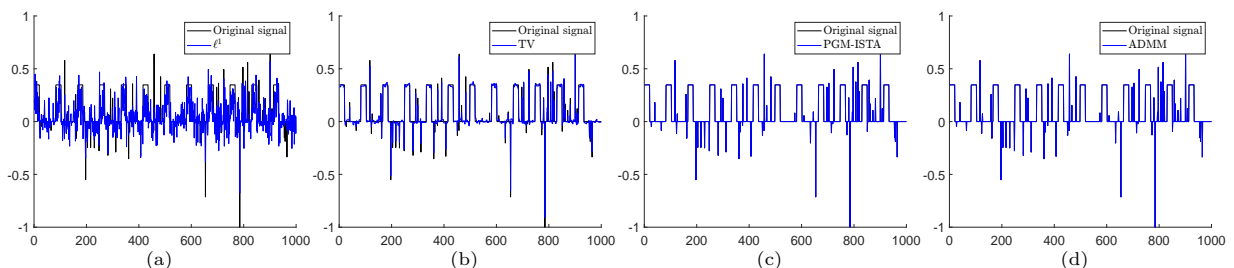


Figure 8: The exact and recovered signals by three methods with a sampling ratio 0.5 and $\sigma = 0$.

5.3 LPGM-ISTA for recovering ECG signals

Last we conduct experiments to recover ECG signals, to illustrate the effectiveness of the ℓ^1 -TV model (1.5) on real-world signals, and compare LPGM-ISTA with traditional iterative algorithms. All experiments of neural networks are performed in Python using PyTorch.

We choose 2372 ECG signals $\{\mathbf{x}_i\}_{i=1}^{2372}$ with length windowed to 256 from the MIT-BIH Arrhythmia Database [44]. The observations are generated by a linear transform as $\mathbf{y}_i = \mathbf{A}\mathbf{x}_i$, where $\mathbf{A} \in \mathbb{R}^{128 \times 256}$ with entries following i.i.d. $\mathcal{N}(0, 1)$. In this way, we obtain the pair of observed signals and its labels $\{(\mathbf{y}_i, \mathbf{x}_i)\}_{i=1}^{2366}$. Next, we choose the first 1900 samples for training, and the remaining 472 samples for testing. The regularization parameters λ_1 and λ_2 are set according to cross-validation, which are verified to satisfy the condition $\lambda_1 + 2\lambda_2 < \lambda_{\max}$. For a typical signal from the test set, we compare the performance of LPGM-ISTA and several existing algorithms for solving problem (1.5) including the proposed PGM-ISTA, LADMM [35], and S-FISTA [7].

We report the relative errors and CPU time in Table 3 with iteration / layer number ranging from 2 to 10 with a step size of 2, and also the results for LADMM, S-FISTA and PGM-ISTA with the iteration number being 500 and 1000. Clearly, LPGM-ISTA far outperforms the three iterative algorithms including LADMM, S-FISTA and the proposed PGM-ISTA in terms of both relative errors and CPU time. The relative errors of LPGM-ISTA show a decreasing trend with the increase of layer / iteration number, and moreover very few layers of the learned algorithm (LPGM-ISTA) are sufficient to achieve satisfactory relative errors compared with the original algorithm, whereas the iterative algorithms lose their effectiveness in terms of the required number of iterations. The exact signal and the recovered ones by the four algorithms with iteration / layer number being 2 are shown in Fig. 9. Most remarkably, LPGM-ISTA can already provide a satisfactory recovery, but LADMM, S-FISTA and PGM-ISTA barely recover any useful information. Thus, LPGM-ISTA does provide a fast solver for problem (1.5). Here the signal length is only 256, which is relatively short. It is expected that the proposed fast learned solver may exhibit greater superiority when dealing with even longer signals.

Table 3: Comparisons of the RelErrs/time (in seconds) of LADMM, S-FISTA, PGM-ISTA and LPGM-ISTA.

Iterations/layers	2	4	6	8	10	500	1000
LADMM [35]	0.8277/-	0.7842/-	0.7615/-	0.7464/-	0.7345/-	0.1386/0.152	0.0391/0.295
S-FISTA [7]	0.8282/-	0.7720/-	0.7427/-	0.7266/-	0.7155/-	0.0712/0.184	0.0502/0.365
PGM-ISTA	0.8255/-	0.7801/-	0.7563/-	0.7413/-	0.7306/-	0.1435/0.204	0.0446/0.364
LPGM-ISTA	0.0560/0.063	0.0503/0.073	0.0435/0.081	0.0413/0.085	0.0391/0.095	-/-	-/-

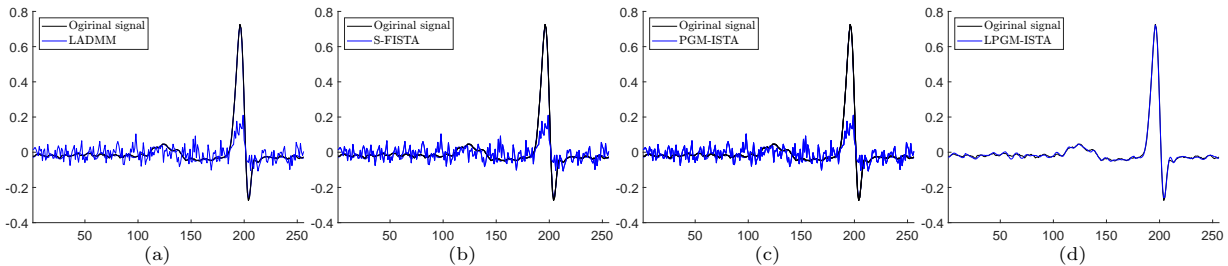


Figure 9: The exact signal and the recovered ones by LADMM, S-FISTA, PGM-ISTA and LPGM-ISTA with iterations/layers being 2.

6 Technical proofs

In this section we give all the technical proofs.

6.1 Proof of Theorem 3.1

The proof is partly inspired from [17]. However, we need to make several essential changes in order to adapt the results to the ℓ^1 -TV case. Technically, we select a vector from the subdifferential of the objective function in (1.4) that yields an upper bound on its statistical dimension. First we give two useful lemmas.

Lemma 6.1 ([53, Grothendieck's identity]). *For any fixed vectors $\mathbf{u}, \mathbf{v} \in \mathbb{S}^{n-1}$, we have*

$$\mathbb{E}_{\mathbf{g} \sim \mathcal{N}(\mathbf{0}, \mathbf{I}_n)}[\text{sign}\langle \mathbf{g}, \mathbf{u} \rangle \text{sign}\langle \mathbf{g}, \mathbf{v} \rangle] = \frac{2}{\pi} \arcsin\langle \mathbf{u}, \mathbf{v} \rangle. \quad (6.1)$$

Lemma 6.2. *Let $\mathbf{D} = [\mathbf{d}_1, \mathbf{d}_2, \dots, \mathbf{d}_{n-1}]^\top$. Then for any $i \in [n-1]$, we have*

$$\mathbb{E}_{\mathbf{g} \sim \mathcal{N}(\mathbf{0}, \mathbf{I}_n)}[(\mathbf{d}_i^\top \text{sign}(\mathbf{g}) \times \text{sign}(\mathbf{d}_i^\top \mathbf{g}))] = 0.$$

Proof. The result follows directly by computing the expectation. \square

Now we can state the proof of Theorem 3.1. Let s_1 and s_2 be the number of adjacent pairs in \mathbb{S}_G and \mathbb{S}_G^c , respectively, with \mathbb{S}_G denoting $\mathbb{S}_G(\mathbf{x})$. That is,

$$s_1 = |\{i \in \{2, 3, \dots, n-1\} : i \in \mathbb{S}_G, i-1 \in \mathbb{S}_G\}|,$$

$$s_2 = |\{i \in \{2, 3, \dots, n-1\} : i \in \mathbb{S}_G^c, i-1 \in \mathbb{S}_G^c\}|.$$

Then $s_1 \leq |\mathbb{S}_G| - 1$ and $s_2 \leq |\mathbb{S}_G^c| - 1$. Since $\partial \|\cdot\|_1(\cdot)$ is a compact set, the following two optimization problems

$$\mathbf{z}_1 = \arg \max_{\mathbf{z} \in \partial \|\cdot\|_1(\mathbf{x})} \langle \mathbf{g}, \mathbf{z} \rangle \quad \text{and} \quad \mathbf{z}_2 = \arg \max_{\mathbf{z} \in \partial \|\cdot\|_1(\mathbf{D}\mathbf{x})} \langle \mathbf{g}, \mathbf{D}^\top \mathbf{z} \rangle$$

are well defined. In addition, we have

$$\begin{aligned} \mathbf{z}_1 &= \arg \max_{\mathbf{z} \in \partial \|\cdot\|_1(\mathbf{x})} \langle \mathbf{g}, \mathbf{z} \rangle = \arg \max_{\|\mathbf{z}\|_\infty \leq 1} \langle \mathbf{g}, \text{sign}(\mathbf{x})_{\mathbb{S}_R} + \mathbf{z}_{\mathbb{S}_R^c} \rangle = \text{sign}(\mathbf{x})_{\mathbb{S}_R} + \text{sign}(\mathbf{g})_{\mathbb{S}_R^c} \\ \mathbf{z}_2 &= \arg \max_{\mathbf{z} \in \partial \|\cdot\|_1(\mathbf{D}\mathbf{x})} \langle \mathbf{g}, \mathbf{D}^\top \mathbf{z} \rangle = \arg \max_{\|\mathbf{z}\|_\infty \leq 1} \langle \mathbf{D}\mathbf{g}, \text{sign}(\mathbf{D}\mathbf{x})_{\mathbb{S}_G} + \mathbf{z}_{\mathbb{S}_G^c} \rangle = \text{sign}(\mathbf{D}\mathbf{x})_{\mathbb{S}_G} + \text{sign}(\mathbf{D}\mathbf{g})_{\mathbb{S}_G^c}. \end{aligned}$$

Consequently,

$$\begin{aligned} \text{dist}^2(\mathbf{g}, t\partial g(\mathbf{x})) &= \text{dist}^2\left(\mathbf{g}, t\lambda_1 \partial \|\cdot\|_1(\mathbf{x}) + t\lambda_2 \mathbf{D}^\top \partial \|\cdot\|_1(\mathbf{D}\mathbf{x})\right) \leq \|\mathbf{g} - t(\lambda_1 \mathbf{z}_1 + \lambda_2 \mathbf{D}^\top \mathbf{z}_2)\|_2^2 \\ &= \|\mathbf{g} - t\lambda_1(\text{sign}(\mathbf{x})_{\mathbb{S}_R} + \text{sign}(\mathbf{g})_{\mathbb{S}_R^c}) - t\lambda_2(\mathbf{D}^\top \text{sign}(\mathbf{D}\mathbf{x})_{\mathbb{S}_G} + \mathbf{D}^\top \text{sign}(\mathbf{D}\mathbf{g})_{\mathbb{S}_G^c})\|_2^2 \\ &= \text{I} + \text{II} + \text{III}, \end{aligned} \tag{6.2}$$

with

$$\begin{aligned} \text{I} &= \|\mathbf{g}\|_2^2 + t^2 \lambda_1^2 (\|\text{sign}(\mathbf{x})_{\mathbb{S}_R}\|_2^2 + \|\text{sign}(\mathbf{g})_{\mathbb{S}_R^c}\|_2^2) + t^2 \lambda_2^2 (\|\mathbf{D}^\top \text{sign}(\mathbf{D}\mathbf{x})_{\mathbb{S}_G}\|_2^2 + \|\mathbf{D}^\top \text{sign}(\mathbf{D}\mathbf{g})_{\mathbb{S}_G^c}\|_2^2), \\ \text{II} &= 2t^2 \lambda_1 \lambda_2 (\langle \text{sign}(\mathbf{g})_{\mathbb{S}_R^c}, \mathbf{D}^\top \text{sign}(\mathbf{D}\mathbf{g})_{\mathbb{S}_G^c} \rangle + \langle \text{sign}(\mathbf{x})_{\mathbb{S}_R}, \mathbf{D}^\top \text{sign}(\mathbf{D}\mathbf{x})_{\mathbb{S}_G} \rangle) \\ &\quad - 2t(\lambda_1 \langle \mathbf{g}, \text{sign}(\mathbf{g})_{\mathbb{S}_R^c} \rangle + \lambda_2 \langle \mathbf{g}, \mathbf{D}^\top \text{sign}(\mathbf{D}\mathbf{g})_{\mathbb{S}_G^c} \rangle), \\ \text{III} &= 2t^2 \lambda_1 \lambda_2 (\langle \text{sign}(\mathbf{x})_{\mathbb{S}_R}, \mathbf{D}^\top \text{sign}(\mathbf{D}\mathbf{g})_{\mathbb{S}_G^c} \rangle + \langle \text{sign}(\mathbf{g})_{\mathbb{S}_R^c}, \mathbf{D}^\top \text{sign}(\mathbf{D}\mathbf{x})_{\mathbb{S}_G} \rangle) \\ &\quad - 2t^2 (\lambda_1^2 \langle \text{sign}(\mathbf{x})_{\mathbb{S}_R}, \text{sign}(\mathbf{g})_{\mathbb{S}_R^c} \rangle + \lambda_2^2 \langle \mathbf{D}^\top \text{sign}(\mathbf{D}\mathbf{x})_{\mathbb{S}_G}, \mathbf{D}^\top \text{sign}(\mathbf{D}\mathbf{g})_{\mathbb{S}_G^c} \rangle) \\ &\quad - 2t(\lambda_1 \langle \mathbf{g}, \text{sign}(\mathbf{x})_{\mathbb{S}_R} \rangle + \lambda_2 \langle \mathbf{g}, \mathbf{D}^\top \text{sign}(\mathbf{D}\mathbf{x})_{\mathbb{S}_G} \rangle). \end{aligned}$$

Taking expectation on both sides of (6.2) gives

$$\mathbb{E}[\text{dist}^2(\mathbf{g}, t\partial g(\mathbf{x}))] \leq \mathbb{E}[\text{I}] + \mathbb{E}[\text{II}] + \mathbb{E}[\text{III}]. \tag{6.3}$$

Next, we bound the terms in (6.3). For the term $\mathbb{E}[\text{I}]$, we have

$$\begin{aligned} \mathbb{E}[\text{I}] &\stackrel{(a)}{=} n + t^2 \left(\lambda_1^2 (|\mathbb{S}_R| + |\mathbb{S}_R^c|) + \lambda_2^2 \sum_{j,k \in \mathbb{S}_G} \mathbf{d}_j^\top \mathbf{d}_k \text{sign}(\mathbf{d}_j^\top \mathbf{x}) \text{sign}(\mathbf{d}_k^\top \mathbf{x}) \right. \\ &\quad \left. + \lambda_2^2 \sum_{j,k \in \mathbb{S}_G^c} \mathbf{d}_j^\top \mathbf{d}_k \frac{2}{\pi} \arcsin \frac{\mathbf{d}_j^\top \mathbf{d}_k}{\|\mathbf{d}_j\|_2 \|\mathbf{d}_k\|_2} \right) \\ &\stackrel{(b)}{\leq} n + t^2 \left(\lambda_1^2 (|\mathbb{S}_R| + |\mathbb{S}_R^c|) + \lambda_2^2 \left(2|\mathbb{S}_G| + 2s_1 + 2|\mathbb{S}_G^c| + \frac{2}{3}s_2 \right) \right) \\ &\leq n + t^2 \left(\lambda_1^2 (|\mathbb{S}_R| + |\mathbb{S}_R^c|) + \lambda_2^2 \left(4|\mathbb{S}_G| + \frac{8}{3}|\mathbb{S}_G^c| - \frac{8}{3} \right) \right), \end{aligned} \tag{6.4}$$

where equality (a) holds, due to the following identities

$$\begin{cases} \mathbb{E}[\|\mathbf{g}\|_2^2] = n, & \mathbb{E}[\|\text{sign}(\mathbf{x})_{\mathbb{S}_R}\|_2^2] = |\mathbb{S}_R|, & \mathbb{E}[\|\text{sign}(\mathbf{g})_{\mathbb{S}_R^c}\|_2^2] = |\mathbb{S}_R^c|, \\ \mathbb{E}[\|\mathbf{D}^\top \text{sign}(\mathbf{D}\mathbf{x})_{\mathbb{S}_G}\|_2^2] = \sum_{j,k \in \mathbb{S}_G} \mathbf{d}_j^\top \mathbf{d}_k \text{sign}(\mathbf{d}_j^\top \mathbf{x}) \text{sign}(\mathbf{d}_k^\top \mathbf{x}), \\ \mathbb{E}[\|\mathbf{D}^\top \text{sign}(\mathbf{D}\mathbf{g})_{\mathbb{S}_G^c}\|_2^2] = \sum_{j,k \in \mathbb{S}_G^c} \mathbf{d}_j^\top \mathbf{d}_k \text{sign}(\mathbf{d}_j^\top \mathbf{g}) \text{sign}(\mathbf{d}_k^\top \mathbf{g}) \stackrel{(c)}{=} \sum_{j,k \in \mathbb{S}_G^c} \mathbf{d}_j^\top \mathbf{d}_k \frac{2}{\pi} \arcsin \frac{\mathbf{d}_j^\top \mathbf{d}_k}{\|\mathbf{d}_j\|_2 \|\mathbf{d}_k\|_2}, \end{cases} \tag{6.5}$$

where (c) is due to Lemma 6.1. The inequality (b) holds since $\mathbf{d}_j^\top \mathbf{d}_k = -1$ if $|j-k|=1$, $\|\mathbf{d}_j\|_2 = \sqrt{2}$ if $j \in [n-1]$ and $\mathbf{d}_j^\top \mathbf{d}_k = 0$ otherwise. For the term $\mathbb{E}[\text{II}]$, we have

$$\mathbb{E}[\text{II}] = 2t^2 \lambda_1 \lambda_2 \left(\sum_{i \in \mathbb{S}_G^c} \mathbb{E} \left[\mathbf{d}_i^\top \text{sign}(\mathbf{g})_{\mathbb{S}_R^c} \times \text{sign}(\mathbf{d}_i^\top \mathbf{g}) \right] + \sum_{i \in \mathbb{S}_G} \mathbf{d}_i^\top \text{sign}(\mathbf{x})_{\mathbb{S}_R} \times \text{sign}(\mathbf{d}_i^\top \mathbf{x}) \right)$$

$$\begin{aligned}
& -2t \left(\lambda_1 \sqrt{\frac{2}{\pi}} |\mathbb{S}_R^c| + \lambda_2 \sqrt{\frac{2}{\pi}} \sum_{i \in \mathbb{S}_G^c} \|\mathbf{d}_i\|_2 \right) \\
& \stackrel{(d)}{\leq} 2t^2 \lambda_1 \lambda_2 (0 + 2 \min\{|\mathbb{S}_R|, |\mathbb{S}_G|\}) - 2\sqrt{\frac{2}{\pi}} t \left(\lambda_1 |\mathbb{S}_R^c| + \lambda_2 \sqrt{2} |\mathbb{S}_G^c| \right) \\
& \leq 4t^2 \lambda_1 \lambda_2 \min\{|\mathbb{S}_R|, |\mathbb{S}_G|\} - 2\sqrt{\frac{2}{\pi}} t \left(\lambda_1 |\mathbb{S}_R^c| + \sqrt{2} \lambda_2 |\mathbb{S}_G^c| \right), \tag{6.6}
\end{aligned}$$

where (d) holds by Lemma 6.2 with $\{i, i+1\} \subset \mathbb{S}_R^c$ or $\{i, i+1\} \subset \mathbb{S}_R$ on the condition $i \in \mathbb{S}_G^c$. For the term $\mathbb{E}[\text{III}]$, we have

$$\mathbb{E}[\text{III}] = 0. \tag{6.7}$$

By substituting (6.4), (6.6) and (6.7) into (6.3), and noting $|\mathbb{S}_R| = s_r$, $|\mathbb{S}_G| = s_g$, $|\mathbb{S}_R^c| = s_r - 1$, $|\mathbb{S}_G^c| = n - 1 - s_g$, we get

$$\begin{aligned}
\text{dist}^2(\mathbf{g}, t\partial g(\mathbf{x})) & \leq \left(\lambda_1^2 (|\mathbb{S}_R| + |\mathbb{S}_R^c|) + \lambda_2^2 \left(4|\mathbb{S}_G| + \frac{8}{3}|\mathbb{S}_G^c| - \frac{8}{3} \right) + 4\lambda_1 \lambda_2 \min\{|\mathbb{S}_R|, |\mathbb{S}_G|\} \right) t^2 \\
& \quad - 2\sqrt{\frac{2}{\pi}} \left(\lambda_1 |\mathbb{S}_R^c| + \sqrt{2} \lambda_2 |\mathbb{S}_G^c| \right) t + n \\
& \leq \left(\lambda_1^2 n + \lambda_2^2 \left(\frac{4}{3}s_g + \frac{8}{3}n - \frac{16}{3} \right) + 4\lambda_1 \lambda_2 \min\{s_r, s_g\} \right) t^2 \\
& \quad - 2\sqrt{\frac{2}{\pi}} \left(\lambda_1 (n - s_r) + \sqrt{2} \lambda_2 (n - 1 - s_g) \right) t + n. \tag{6.8}
\end{aligned}$$

Meanwhile, by [18], we have

$$\delta(\mathcal{D}(g, \mathbf{x})) \leq \inf_{t \geq 0} \mathbb{E}[\text{dist}^2(\mathbf{g}, t\partial g(\mathbf{x}))]. \tag{6.9}$$

By minimizing (6.8) in t and combining with (6.9), we get

$$\delta(\mathcal{D}(g, \mathbf{x})) \leq n - \frac{6}{\pi} \frac{[\lambda_1 (n - s_r) + \sqrt{2} \lambda_2 (n - 1 - s_g)]^2}{3n\lambda_1^2 + 4(2n + s_g - 4)\lambda_2^2 + 12\lambda_1 \lambda_2 \min\{s_r, s_g\}} = \Phi(s_r, s_g).$$

This completes the proof of the theorem.

6.2 Proof of Theorem 3.2

Proof. By [52, Corollary 3.5], we have that with a probability at least $1 - e^{-\frac{t^2}{2}}$, there holds

$$\|\mathbf{x}^* - \hat{\mathbf{x}}\|_2 \leq \frac{2\epsilon}{[\sqrt{m-1} - w(\mathcal{D}(g, \mathbf{x}^*)) - t]_+}. \tag{6.10}$$

In addition, Remark 1 of Theorem 3.1 implies $w(\mathcal{D}(g, \mathbf{x}^*)) \leq \sqrt{\Phi(s_r, s_g)}$. By substituting it into (6.10), and combining with the assumption $m > (\sqrt{\Phi(s_r, s_g)} + t)^2 + 1$, we complete the proof. \square

6.3 Proof of Theorem 4.1

First we outline the overall proof strategy. For part (a), we first show that there exists (u, t) such that $\mathcal{G}_{1/u}^{f, g_1}(\mathbf{x}^k(u, t)) \in \partial F_1(\mathbf{x}^k(u, t))$, and then Algorithm 1 can be viewed as the proximal subgradient method [5], whose global convergence is guaranteed. Part (b) is proved by showing that the sequence $\{\mathbf{x}^k\}_{k \geq 0}$ generated by Algorithm 1 is Fejér monotone, which converges to some fixed points. First we give a useful lemma.

Lemma 6.3. *Let $\mathbf{x} \in \mathbb{R}^n$, $\mathbf{A} = [\mathbf{a}_1, \mathbf{a}_2, \dots, \mathbf{a}_n]$ and $\mathbb{I}_{\neq}(\mathbf{x}) = \{i | x_i \neq 0, i \in [n]\}$. Suppose that $u_0 > 0$ satisfies*

$$\frac{1}{u_0} \geq \max \left\{ \frac{\text{sign}(x_i) \lambda_1 + \sum_{j=1}^n \mathbf{a}_i^\top \mathbf{a}_j x_j - \mathbf{a}_i^\top \mathbf{y}}{x_i}, i \in \mathbb{I}_{\neq}(\mathbf{x}) \right\}. \tag{6.11}$$

Then, for any $u \in (0, u_0]$,

$$\mathcal{G}_{1/u}^{f, g_1}(\mathbf{x}) \subset \partial F_1(\mathbf{x}), \tag{6.12}$$

where $F_1(\mathbf{x}) = f(\mathbf{x}) + g_1(\mathbf{x})$ with $f(\mathbf{x}) = \frac{1}{2} \|\mathbf{y} - \mathbf{A}\mathbf{x}\|_2^2$ and $g_1(\mathbf{x}) = \lambda_1 \|\mathbf{x}\|_1$.

Proof. The i -th coordinate of $\partial F_1(\mathbf{x})$ is

$$[\partial F_1(\mathbf{x})]_i \in \begin{cases} [\nabla f(\mathbf{x})]_i + \lambda_1, & x_i > 0 \\ [\nabla f(\mathbf{x})]_i + [-\lambda_1, \lambda_1], & x_i = 0 \\ [\nabla f(\mathbf{x})]_i - \lambda_1, & x_i < 0 \end{cases} \quad (6.13)$$

Moreover,

$$\begin{aligned} \mathcal{G}_{1/u}^{f,g_1}(\mathbf{x}) &= \frac{1}{u} (\mathbf{x} - \text{prox}_{ug_1}(\mathbf{x} - u\nabla f(\mathbf{x}))) \\ &= \frac{1}{u} (\mathbf{x} - \text{sign}(\mathbf{x} - u\nabla f(\mathbf{x})) \odot [|\mathbf{x} - u\nabla f(\mathbf{x})| - \lambda_1 u]_+). \end{aligned}$$

Hence, the i -th coordinate of $\mathcal{G}_{1/u}^{f,g_1}(\mathbf{x})$ is

$$[\mathcal{G}_{1/u}^{f,g_1}(\mathbf{x})]_i \in \begin{cases} [\nabla f(\mathbf{x})]_i + \lambda_1, & [\frac{1}{u}\mathbf{x} - \nabla f(\mathbf{x})]_i \geq \lambda_1 \\ [\nabla f(\mathbf{x})]_i + (-\lambda_1, \lambda_1), & [\frac{1}{u}\mathbf{x} - \nabla f(\mathbf{x})]_i \in (-\lambda_1, \lambda_1) \\ [\nabla f(\mathbf{x})]_i - \lambda_1, & [\frac{1}{u}\mathbf{x} - \nabla f(\mathbf{x})]_i \leq -\lambda_1 \end{cases} \quad (6.14)$$

Thus, if $x_i \in \mathbb{I}_0(\mathbf{x}) = \{i | x_i = 0, i \in [n]\}$, it follows from (6.13) and (6.14) that

$$[\mathcal{G}_{1/u}^{f,g_1}(\mathbf{x})]_i \subset [\partial F_1(\mathbf{x})]_i. \quad (6.15)$$

If $x_i > 0$, it follows from (6.11) that

$$\frac{1}{u} \geq \frac{1}{u_0} \geq \frac{\lambda_1 + \sum_{j=1}^n \mathbf{a}_i^\top \mathbf{a}_j x_j - \mathbf{a}_i^\top \mathbf{y}}{x_i},$$

which implies

$$[\frac{1}{u}\mathbf{x} - \nabla f(\mathbf{x})]_i \geq \lambda_1. \quad (6.16)$$

Combining (6.13) and (6.16) gives

$$[\mathcal{G}_{1/u}^{f,g_1}(\mathbf{x})]_i = [\partial F_1(\mathbf{x})]_i. \quad (6.17)$$

Similarly, if $x_i < 0$, repeating the argument for $x_i > 0$ implies that (6.17) also holds for $u \in (0, u_0]$. Combining (6.15) and (6.17) gives (6.12). \square

Lemma 6.3 indicates $\mathcal{G}_{1/u}^{f,g_1}(\mathbf{x}) \subset \partial F_1(\mathbf{x})$ for suitable u , connecting the proposed algorithms with the proximal subgradient method [5].

Proof of Theorem 4.1. Part (a). We first claim that for any integer $k \geq 0$, there exist $u > 0$ and $t > 0$, such that the sequence $\{\mathbf{x}^k(u, t)\}_{k \geq 0}$ satisfies

$$\mathcal{G}_{1/u}^{f,g_1}(\mathbf{x}^k(u, t)) \in \partial F_1(\mathbf{x}^k(u, t)). \quad (6.18)$$

The proof of (6.18) will be given later. The relation (6.18) implies that Algorithm 1 can be viewed as the proximal subgradient method [5]. Following the theory of the proximal subgradient method, there exists a constant step size $t > 0$ satisfying $\mathbf{x}(u, t) = \mathbf{x}^*$ and

$$\mathbf{x}(u, t) = \text{prox}_{tg_2}(\mathbf{x}(u, t) - t\mathcal{G}_{1/u}^{f,g_1}(\mathbf{x}(u, t))). \quad (6.19)$$

Next, we prove (6.18) by mathematical induction. For $k = 0, 1$, by Lemma 6.3, there exist $u_0, u_1 \in (0, \infty)$ satisfying (6.11) for \mathbf{x}^0 and \mathbf{x}^1 respectively, and for any $u' \in (0, u_0]$, $u'' \in (0, u_1]$,

$$\mathcal{G}_{1/u'}^{f,g_1}(\mathbf{x}^0) \in \partial F_1(\mathbf{x}^0) \quad \text{and} \quad \mathcal{G}_{1/u''}^{f,g_1}(\mathbf{x}^1) \in \partial F_1(\mathbf{x}^1).$$

Choosing $u = \min\{u_0, u_1\}$ leads to

$$\mathcal{G}_{1/u}^{f,g_1}(\mathbf{x}^0) \in \partial F_1(\mathbf{x}^0) \quad \text{and} \quad \mathcal{G}_{1/u}^{f,g_1}(\mathbf{x}^1) \in \partial F_1(\mathbf{x}^1).$$

Suppose that for an integer $k \geq 0$, $\mathcal{G}_{1/u}^{f,g_1}(\{\mathbf{x}^k\}) \in \partial F_1(\{\mathbf{x}^k\})$, by induction, the above arguments indicate that we can always find $u > 0$ so that $\mathcal{G}_{1/u}^{f,g_1}(\{\mathbf{x}^{k+1}\}) \in \partial F_1(\{\mathbf{x}^{k+1}\})$, which implies the claim (6.18).

Part (b). The proof of part (a) indicates that a small parameter pair (u, t) can ensure the convergence. Hence, we can choose (u, t) with $u \in (0, 2/\|\mathbf{A}\|_2^2)$ and $t \in (0, u]$ which also implies the convergence of Algorithm 1. That is, (6.19) holds for some $\mathbf{x}(u_0, t_0) = \mathbf{x}^*$ with $u_0 \in (0, 2/\|\mathbf{A}\|_2^2)$ and $t_0 \in (0, u_0]$. For any $k \geq 0$, upon letting $\mathbf{x}^k(u, t) = \mathbf{x}^k$, we have

$$\begin{aligned}
\|\mathbf{x}^{k+1} - \mathbf{x}^*\|_2 &= \left\| \text{prox}_{t g_2} \left(\mathbf{x}^k - t \mathcal{G}_{1/u}^{f, g_1}(\mathbf{x}^k) \right) - \text{prox}_{t g_2} \left(\mathbf{x}^* - t \mathcal{G}_{1/u}^{f, g_1}(\mathbf{x}^*) \right) \right\|_2 \\
&\stackrel{(a)}{\leq} \left\| (\mathbf{x}^k - \mathbf{x}^*) - t \left(\mathcal{G}_{1/u}^{f, g_1}(\mathbf{x}^k) - \mathcal{G}_{1/u}^{f, g_1}(\mathbf{x}^*) \right) \right\|_2 \\
&\stackrel{(b)}{\leq} \frac{t}{u} \left\| \text{prox}_{u g_1} \left(\mathbf{x}^k - u \mathbf{A}^\top (\mathbf{A} \mathbf{x}^k - \mathbf{y}) \right) - \text{prox}_{u g_1} \left(\mathbf{x}^* - u \mathbf{A}^\top (\mathbf{A} \mathbf{x}^* - \mathbf{y}) \right) \right\|_2 \\
&\quad + \left| 1 - \frac{t}{u} \right| \cdot \|\mathbf{x}^k - \mathbf{x}^*\|_2 \\
&\stackrel{(c)}{\leq} \frac{t}{u} \left\| (\mathbf{I}_n - u \mathbf{A}^\top \mathbf{A}) (\mathbf{x}^k - \mathbf{x}^*) \right\|_2^2 + \left| 1 - \frac{t}{u} \right| \cdot \|\mathbf{x}^k - \mathbf{x}^*\|_2 \\
&\stackrel{(d)}{\leq} \rho(u, t) \|\mathbf{x}^k - \mathbf{x}^*\|_2, \tag{6.20}
\end{aligned}$$

where $\rho(u, t) = |1 - \frac{t}{u}| + \frac{t}{u} \|\mathbf{I}_n - u \mathbf{A}^\top \mathbf{A}\|_2$, (a) and (c) hold by the nonexpansivity of the proximal operator [5, Theorem 6.42], and (b) and (d) hold by the triangular inequality. Since $u \in (0, 2/\|\mathbf{A}\|_2^2)$, $t \in (0, u]$, we get $\rho(u, t) = 1 - \frac{t}{u} + \frac{t}{u} \|\mathbf{I}_n - u \mathbf{A}^\top \mathbf{A}\|_2$. Further, since $\|\mathbf{I}_n - u \mathbf{A}^\top \mathbf{A}\|_2 = \|u \mathbf{A}^\top \mathbf{A} - \mathbf{I}_n\|_2$, we obtain

$$\begin{aligned}
\|\mathbf{I}_n - u \mathbf{A}^\top \mathbf{A}\|_2 &= \max_{\mathbf{x} \in \mathbb{S}^{n-1}} \langle (\mathbf{I}_n - u \mathbf{A}^\top \mathbf{A}) \mathbf{x}, \mathbf{x} \rangle \\
&= \max_{\mathbf{x} \in \mathbb{S}^{n-1}} |1 - u \|\mathbf{A} \mathbf{x}\|_2^2| = \max\{|1 - u s_n^2|, |1 - u s_1^2|\},
\end{aligned}$$

where s_1 and s_n are the maximal and minimal singular values of \mathbf{A} and the last equality holds since $s_n^2 \leq \|\mathbf{A} \mathbf{x}\|_2^2 \leq s_1^2$. Since $\mathbf{A} \in \mathbb{R}^{m \times n}$ with $m < n$, we obtain $s_n = 0$. Thus for $u \in (0, 2/\|\mathbf{A}\|_2^2)$, $\|\mathbf{I}_n - u \mathbf{A}^\top \mathbf{A}\|_2 = \max\{1, |1 - u s_1^2|\} = 1$. These discussions imply $\rho(u, t) = 1$. By substituting the identity into (6.20), we get

$$\|\mathbf{x}^{k+1} - \mathbf{x}^*\|_2 \leq \|\mathbf{x}^k - \mathbf{x}^*\|_2. \tag{6.21}$$

This estimate implies that the sequence $\{\mathbf{x}^k\}_{k \geq 0}$ generated by Algorithm 1 is Fejér monotone and hence converges to some fixed points [5, Theorem 8.16]. \square

6.4 Proof of Theorem 4.2

First we describe the overall proof strategy. We first construct a $4/(3u)$ -smooth function $H_u(\cdot)$ to obtain $F_u(\cdot) = H_u(\cdot) + g_2(\cdot)$. Then $F_u(\cdot)$ is used to approximate $F(\cdot)$, which yields an upper bound of $F(\mathbf{x}^{k+1}) - F(\mathbf{x}^*)$. Below we denote $f(\mathbf{x}) = \frac{1}{2} \mathbf{x}^\top \mathbf{Q} \mathbf{x} + \mathbf{b}^\top \mathbf{x} + c$, with $\mathbf{Q} = \mathbf{A}^\top \mathbf{A}$, $\mathbf{b} = \mathbf{A}^\top \mathbf{y}$ and $c = \frac{1}{2} \mathbf{y}^\top \mathbf{y}$. We denote by l_f , l_{g_1} and l_{g_2} the Lipschitz constants of $f(\cdot)$, $g_1(\cdot)$ and $g_2(\cdot)$. To prove Theorem 4.2, we need the next lemma on the gradient mapping operator.

Lemma 6.4 ([49, Lemma 2.1]). *For any $u > 0$ and $\mathbf{x} \in \mathbb{R}^n$,*

$$\left\| \mathcal{G}_{1/u}^{f, g_1}(\mathbf{x}) \right\|_2 \leq \|\mathbf{Q}\|_2 r + \|\mathbf{b}\|_2 + l_{g_1}.$$

Now, we are ready to prove Theorem 4.2.

Proof of Theorem 4.2. Consider the function $H_u : \mathbb{R}^n \rightarrow \mathbb{R}$ given by

$$H_u(\mathbf{x}) = \frac{1}{2} \mathbf{x}^\top (\mathbf{Q} - u \mathbf{Q}^2) \mathbf{x} - \mathbf{b}^\top (\mathbf{I}_n - u \mathbf{Q}) \mathbf{x} + M_{g_1}^u((\mathbf{I}_n - u \mathbf{Q}) \mathbf{x} + u \mathbf{b}) + \frac{1}{2} \mathbf{y}^\top \mathbf{y},$$

where $M_{g_1}^u$ is the Moreau envelope of g_1 with a smoothness parameter u (see [45] for Moreau envelope). Note that H_u is convex since $u \in (0, 2/\|\mathbf{Q}\|_2)$ and the Moreau envelope of a convex function is convex. Since the gradient of the Moreau envelope is given by $\nabla M_{g_1}^u(\mathbf{x}) = \frac{1}{u}(\mathbf{x} - \text{prox}_{u g_1}(\mathbf{x}))$, we have

$$\nabla H_u(\mathbf{x}) = (\mathbf{I}_n - u \mathbf{Q}) \mathcal{G}_{1/u}^{f, g_1}(\mathbf{x}). \tag{6.22}$$

Let $\mathbf{a}_1 = \frac{1}{t}(\mathbf{x}^k - \text{prox}_{t g_2}(\mathbf{x}^k - t \nabla H_u(\mathbf{x}^k))) = \mathcal{G}_{1/t}^{H_u, g_2}(\mathbf{x}^k)$ and $\mathbf{a}_2 = \frac{1}{t}(\mathbf{x}^k - \text{prox}_{t g_2}(\mathbf{x}^k - t \mathcal{G}_{1/u}^{f, g_1}(\mathbf{x}^k))) = \frac{1}{t}(\mathbf{x}^k - \mathbf{x}^{k+1})$. Then by the triangle inequality, we have

$$\|\mathbf{a}_1\|_2 \leq \|\mathbf{a}_2\|_2 + \|\mathbf{a}_1 - \mathbf{a}_2\|_2. \tag{6.23}$$

Next, by (6.22) and nonexpansivity of the proximal operator [5, Theorem 6.42], and Lemma 6.4, we have

$$\begin{aligned}\|\mathbf{a}_1 - \mathbf{a}_2\|_2 &= \frac{1}{t} \left\| \text{prox}_{t g_2}(\mathbf{x}^k - t \nabla H_u(\mathbf{x}^k)) - \text{prox}_{t g_2}(\mathbf{x}^k - t \mathcal{G}_{1/u}^{f, g_1}(\mathbf{x}^k)) \right\|_2 \\ &\leq \left\| (\mathbf{I}_n - u \mathbf{Q}) \mathcal{G}_{1/u}^{f, g_1}(\mathbf{x}^k) - \mathcal{G}_{1/u}^{f, g_1}(\mathbf{x}^k) \right\|_2 = u \left\| \mathbf{Q} \mathcal{G}_{1/u}^{f, g_1}(\mathbf{x}^k) \right\|_2 \\ &\leq u \|\mathbf{Q}\|_2 (\|\mathbf{Q}\|_2 r + \|\mathbf{b}\|_2 + l_{g_1})?\end{aligned}\tag{6.24}$$

By assumption (3.6), we have

$$\|\mathbf{a}_2\|_2 = \frac{1}{t} \|\mathbf{x}^k - \mathbf{x}^{k+1}\|_2 \leq \epsilon.\tag{6.25}$$

By combining (6.23), (6.24) and (6.25), we get

$$\|\mathbf{a}_1\|_2 = \|\mathcal{G}_{1/t}^{H_u, g_2}(\mathbf{x}^k)\|_2 \leq \epsilon + u \|\mathbf{Q}\|_2 (\|\mathbf{Q}\|_2 r + \|\mathbf{b}\|_2 + l_{g_1}).\tag{6.26}$$

Further, for any $\mathbf{x}_1, \mathbf{x}_2 \in \mathbb{R}^n$, we have

$$\begin{aligned}\|\nabla H_u(\mathbf{x}_1) - \nabla H_u(\mathbf{x}_2)\|_2 &= \left\| (\mathbf{I}_n - u \mathbf{Q}) \left(\mathcal{G}_{1/u}^{f, g_1}(\mathbf{x}_1) - \mathcal{G}_{1/u}^{f, g_1}(\mathbf{x}_2) \right) \right\|_2 \\ &\leq \left\| \mathcal{G}_{1/u}^{f, g_1}(\mathbf{x}_1) - \mathcal{G}_{1/u}^{f, g_1}(\mathbf{x}_2) \right\|_2 \leq \frac{4}{3u} \|\mathbf{x}_1 - \mathbf{x}_2\|_2,\end{aligned}$$

where the first line holds since $u \in (0, 2/\|\mathbf{Q}\|_2)$ and the second line holds since gradient mapping operators are firmly non-expansive with constant $3u/4$ [5, Lemma 10.11] (i.e., $H_u(\cdot)$ is $4/(3u)$ -smooth, cf. Definition 2.6 for l -smooth). Denote $F_u(\mathbf{x}) = H_u(\mathbf{x}) + g_2(\mathbf{x})$ and a minimizer by $\mathbf{x}_u^* \in \arg \min_{\mathbf{x}} F_u(\mathbf{x})$. Moreover, define

$$\hat{\mathbf{x}}_u = \text{prox}_{t g_2}(\mathbf{x}^k - t \nabla H_u(\mathbf{x}^k)).$$

By the fundamental prox-grad inequality [5, Theorem 10.16], the convexity of $H_u(\cdot)$ and the three-points lemma [12], since $t \in (0, 3u/4)$, it follows that

$$\begin{aligned}F_u(\mathbf{x}_u^*) - F_u(\hat{\mathbf{x}}_u) &\geq \frac{1}{2t} \|\mathbf{x}_u^* - \hat{\mathbf{x}}_u\|_2^2 - \frac{1}{2t} \|\mathbf{x}_u^* - \mathbf{x}^k\|_2^2 \\ &= \frac{1}{2t} (2 \langle \mathbf{x}^k - \hat{\mathbf{x}}_u, \mathbf{x}_u^* - \hat{\mathbf{x}}_u \rangle - \|\mathbf{x}^k - \hat{\mathbf{x}}_u\|_2^2),\end{aligned}$$

Thus, by the Cauchy-Schwarz inequality and the estimate $\|\mathbf{x}^k - \mathbf{x}_u^*\|_2 \leq 2r$,

$$\begin{aligned}F_u(\hat{\mathbf{x}}_u) - F_u(\mathbf{x}_u^*) &\leq \frac{1}{2t} \|\mathbf{x}^k - \hat{\mathbf{x}}_u\|_2^2 + \frac{1}{t} \langle \hat{\mathbf{x}}_u - \mathbf{x}_u^*, \mathbf{x}^k - \hat{\mathbf{x}}_u \rangle \\ &= -\frac{1}{2t} \|\mathbf{x}^k - \hat{\mathbf{x}}_u\|_2^2 + \frac{1}{t} \langle \mathbf{x}^k - \mathbf{x}_u^*, \mathbf{x}^k - \hat{\mathbf{x}}_u \rangle \\ &= -\frac{1}{2t} \|\mathbf{x}^k - \mathbf{x}_u^*\|_2^2 + \langle \mathbf{x}^k - \mathbf{x}_u^*, \mathcal{G}_{1/t}^{H_u, g_2}(\mathbf{x}^k) \rangle \\ &\leq \langle \mathbf{x}^k - \mathbf{x}_u^*, \mathcal{G}_{1/t}^{H_u, g_2}(\mathbf{x}^k) \rangle \leq 2r \left\| \mathcal{G}_{1/t}^{H_u, g_2}(\mathbf{x}^k) \right\|_2\end{aligned}\tag{6.27}$$

Combining (6.26) with (6.27) yields

$$F_u(\hat{\mathbf{x}}_u) - F_u(\mathbf{x}_u^*) \leq 2r\epsilon + 2ur \|\mathbf{Q}\|_2 (\|\mathbf{Q}\|_2 r + \|\mathbf{b}\|_2 + l_{g_1}).\tag{6.28}$$

Finally, we connect $F_u(\mathbf{x}_u^*)$, $F_u(\mathbf{x}^k)$ with $F(\mathbf{x}_u^*)$, $F(\mathbf{x}^k)$, respectively. Note that for any $\mathbf{x} \in \mathbb{R}^n$, by basic properties of the Moreau envelope [5, Theorem 10.51] in (6.29) and the l_{g_1} -Lipschitz property of g_1 , we have

$$\begin{aligned}|H_u(\mathbf{x}) - f(\mathbf{x}) - g_1(\mathbf{x})| &= \left| u \left(-\frac{1}{2} \|\mathbf{Q} \mathbf{x}\|_2^2 + \mathbf{b}^\top \mathbf{Q} \mathbf{x} \right) + M_{g_1}^u((\mathbf{I}_n - u \mathbf{Q}) \mathbf{x} + u \mathbf{b}) - g_1(\mathbf{x}) \right| \\ &\leq \left(\frac{1}{2} \|\mathbf{Q}\|_2^2 r^2 + \|\mathbf{b}\|_2 \|\mathbf{Q}\|_2 r \right) u + |M_{g_1}^u((\mathbf{I}_n - u \mathbf{Q}) \mathbf{x} + u \mathbf{b}) - g_1(\mathbf{x})| \\ &\leq \left(\frac{1}{2} \|\mathbf{Q}\|_2^2 r^2 + \|\mathbf{b}\|_2 \|\mathbf{Q}\|_2 r \right) u + |M_{g_1}^u((\mathbf{I}_n - u \mathbf{Q}) \mathbf{x} + u \mathbf{b}) \\ &\quad - g_1((\mathbf{I}_n - u \mathbf{Q}) \mathbf{x} + u \mathbf{b})| + |g_1((\mathbf{I}_n - u \mathbf{Q}) \mathbf{x} + u \mathbf{b}) - g_1(\mathbf{x})| \\ &\leq \left(\frac{1}{2} \|\mathbf{Q}\|_2^2 r^2 + \|\mathbf{b}\|_2 \|\mathbf{Q}\|_2 r \right) u + \frac{l_{g_1}^2}{2} u + l_{g_1} (\|\mathbf{Q}\|_2 r + \|\mathbf{b}\|_2) u \\ &\leq (\|\mathbf{Q}\|_2 r + \|\mathbf{b}\|_2) (\|\mathbf{Q}\|_2 r + l_{g_1}) u + \frac{l_{g_1}^2}{2} u.\end{aligned}\tag{6.29}$$

Thus, we obtain $|H_u(\mathbf{x}) - f(\mathbf{x}) - g_1(\mathbf{x})| = |F_u(\mathbf{x}) - F(\mathbf{x})| \leq cu$, with $c = (\|\mathbf{Q}\|_{2r} + \|\mathbf{b}\|_2)(\|\mathbf{Q}\|_{2r} + l_{g_1}) + \frac{l_{g_1}^2}{2}$. Consequently,

$$\min_{\mathbf{x}} F(\mathbf{x}) \geq \min_{\mathbf{x}} F_u(\mathbf{x}) - cu, \quad \text{i.e.,} \quad F(\mathbf{x}^*) \geq F_u(\mathbf{x}_u^*) - cu. \quad (6.30)$$

Moreover, since $\|\mathbf{x}^{k+1} - \hat{\mathbf{x}}_u\|_2 = t\|\mathbf{a}_1 - \mathbf{a}_2\|_2$, we have

$$\begin{aligned} F(\mathbf{x}^{k+1}) - F(\hat{\mathbf{x}}_u) &\leq |f(\mathbf{x}^{k+1}) - f(\hat{\mathbf{x}}_u)| + |g_1(\mathbf{x}^{k+1}) - g_1(\hat{\mathbf{x}}_u)| + |g_2(\mathbf{x}^{k+1}) - g_2(\hat{\mathbf{x}}_u)| \\ &\leq (l_f + l_{g_1} + l_{g_2}) \|\mathbf{x}^{k+1} - \hat{\mathbf{x}}_u\|_2 = (l_f + l_{g_1} + l_{g_2}) t \|\mathbf{a}_1 - \mathbf{a}_2\|_2. \end{aligned}$$

Combining this with (6.24) leads to

$$F(\mathbf{x}^{k+1}) \leq F(\hat{\mathbf{x}}_u) + t\kappa u, \quad (6.31)$$

with $\kappa = (l_f + l_{g_1} + l_{g_2}) \|\mathbf{Q}\|_2 (\|\mathbf{Q}\|_{2r} + \|\mathbf{b}\|_2 + l_{g_1})$. Finally, combining (6.28), (6.30) and (6.31) gives

$$F(\mathbf{x}^{k+1}) - F(\mathbf{x}^*) \leq 2r\epsilon + (2r\|\mathbf{Q}\|_2 (\|\mathbf{Q}\|_{2r} + \|\mathbf{b}\|_2 + l_{g_1}) + t\kappa + c)u = 2r\epsilon + (t\kappa + \beta)u. \quad (6.32)$$

By [5, Theorem 3.61] (for Lipschitz functions), we can choose $l_f = \|\mathbf{Q}\|_{2r} + \|\mathbf{b}\|_2$. Obviously, $g_1(\cdot)$ and $g_2(\cdot)$ are Lipschitz with $l_{g_1} = \lambda_1$ and $l_{g_2} = \lambda_2 \|\mathbf{D}\|_2$. Substituting them into (6.32) completes the proof. \square

7 Conclusion and discussions

Motivated by the ℓ^1 and TV penalties in compressed sensing, we have investigated the ℓ^1 -TV method, which simultaneously enforces sparsity and gradient sparsity in the signal. We have established the recovery guarantee of the ℓ^1 -TV method, which quantifies the required number of measurements depending on regular sparsity and gradient sparsity levels in order to achieve successful recovery. We have proposed the PGM-ISTA algorithm based on the gradient mapping and proximal operator, and analyzed theoretical properties of PGM-ISTA, including global convergence and its parameter selections. In addition, we have proposed a learned solver for the regularized problem, by unrolling the PGM-ISTA. The experimental results on ECG signals show that LPGM-ISTA significantly outperforms traditional algorithms.

Below we briefly discuss several topics that are pertinent to this work as well as future research topics.

Combination of regularizers. In many recovery problems, combined regularizers have shown enhanced recovery performance. The theoretical research, however, lags far behind, impeding its interpretability and practical applications. Our findings provide a robust recovery guarantee for the ℓ^1 -TV method, thereby stimulating further research on recovery problems using combined convex regularizers.

Equivalence between constrained problem (1.4) and the regularized problem (1.5). Theoretical guarantees for the constrained form like (1.4) seem preferred, but numerical algorithms are mostly designed for the regularized counterparts like (1.5). Several recent studies have investigated the equivalence between the constrained problem and its regularized counterpart in some special cases [34, 57]. However, existing studies fall far short in providing a general equivalence. Thus, it requires further research to expound the equivalence between problems (1.4) and (1.5).

Relationship with fused LASSO. The model (1.5) resembles the fused LASSO (FLASSO) in statistics. Since combining ℓ^1 and TV regularizers is efficient in inducing sparsity and gradient sparsity in signals, FLASSO has been widely applied in classification and coefficient selection [35, 51, 46]. These successful applications confirm the benefit of combining ℓ^1 and TV regularizers in the context of CS. The proposed LPGM-ISTA can be directly applied to solve the FLASSO problem.

Theoretical perspectives of LPGM-ISTA. In contrast to successful practical applications of algorithm unrolling, its theoretical understanding is still in its nascent stage. Recently, Chen et al. [13, 37] proved that LISTA can attain a linear convergence, which is better than the sublinear convergence of ISTA/FISTA in general scenarios. Their research findings can shed insights into the theoretical underpinnings of LPGM-ISTA.

Acknowledgements

This research was funded by National Natural Science Foundation of China (Grants No. 12301594, 12071380), National Key Research and Development Program of China (Grant No. 2023YFA1008500), Joint Funds of the Natural Science Innovation-Driven Development of Chongqing (Grant No. 2023NSCQ-LZX0218), Sichuan Science and Technology Program (Grant No. 2023NSFSCO060).

Data availability statement

Our code is available at <https://github.com/fsluixl/LGPM-ISTA>

References

- [1] D. Amelunxen, M. Lotz, M. B. McCoy, and J. A. Tropp. Living on the edge: phase transitions in convex programs with random data. *Inf. Inference*, 3(3):224–294, 2014.
- [2] D. Angelosante, G. B. Giannakis, and E. Grossi. Compressed sensing of time-varying signals. In *16th International Conference on Digital Signal Processing*, pages 1–8, 2009.
- [3] S. W. Anzengruber and R. Ramlau. Morozov’s discrepancy principle for Tikhonov-type functionals with nonlinear operators. *Inverse Problems*, 26(2):025001, 17, 2010.
- [4] R. Barbano, v. Z. Kereta, A. Hauptmann, S. R. Arridge, and B. Jin. Unsupervised knowledge-transfer for learned image reconstruction. *Inverse Problems*, 38(10):104004, 28, 2022.
- [5] A. Beck. *First-order methods in optimization*. SIAM, Philadelphia, PA, 2017.
- [6] A. Beck and M. Teboulle. A fast iterative shrinkage-thresholding algorithm for linear inverse problems. *SIAM J. Imaging Sci.*, 2(1):183–202, 2009.
- [7] A. Beck and M. Teboulle. Smoothing and first order methods: a unified framework. *SIAM J. Optim.*, 22(2):557–580, 2012.
- [8] S. Boyd, N. Parikh, E. Chu, B. Peleato, and J. Eckstein. Distributed optimization and statistical learning via the alternating direction method of multipliers. *Foundations and Trends[®] in Machine learning*, 3(1):1–122, 2011.
- [9] J.-F. Cai and W. Xu. Guarantees of total variation minimization for signal recovery. *Inf. Inference*, 4(4):328–353, 2015.
- [10] E. J. Candès, Y. C. Eldar, D. Needell, and P. Randall. Compressed sensing with coherent and redundant dictionaries. *Appl. Comput. Harmon. Anal.*, 31(1):59–73, 2011.
- [11] E. J. Candès, J. Romberg, and T. Tao. Robust uncertainty principles: exact signal reconstruction from highly incomplete frequency information. *IEEE Trans. Inform. Theory*, 52(2):489–509, 2006.
- [12] G. Chen and M. Teboulle. Convergence analysis of a proximal-like minimization algorithm using Bregman functions. *SIAM J. Optim.*, 3(3):538–543, 1993.
- [13] X. Chen, J. Liu, Z. Wang, and W. Yin. Theoretical linear convergence of unfolded ISTA and its practical weights and thresholds. In *Advances in Neural Information Processing Systems*, pages 9079–9089, 2018.
- [14] H. Cherkaoui, J. Sulam, and T. Moreau. Learning to solve TV regularized problems with unrolled algorithms. In *Advances in Neural Information Processing Systems (NeurIPS)*, pages 11513–11524, 2020.
- [15] L. Condat. A direct algorithm for 1-d total variation denoising. *IEEE Signal Proc. Lett.*, 20(11):1054–1057, 2013.
- [16] L. Cui, L. Bai, Y. Wang, P. S. Yu, and E. R. Hancock. Fused lasso for feature selection using structural information. *Pattern Recogn.*, 119:108058, 2021.
- [17] S. Daei, F. Haddadi, and A. Amini. Sample complexity of total variation minimization. *IEEE Signal Proc. Lett.*, 25(8):1151–1155, 2018.
- [18] S. Daei, F. Haddadi, A. Amini, and M. Lotz. On the error in phase transition computations for compressed sensing. *IEEE Trans. Inform. Theory*, 65(10):6620–6632, 2019.
- [19] I. Daubechies, M. Defrise, and C. De Mol. An iterative thresholding algorithm for linear inverse problems with a sparsity constraint. *Comm. Pure Appl. Math.*, 57(11):1413–1457, 2004.
- [20] D. L. Donoho. Compressed sensing. *IEEE Trans. Inform. Theory*, 52(4):1289–1306, 2006.
- [21] D. L. Donoho. For most large underdetermined systems of linear equations the minimal l_1 -norm solution is also the sparsest solution. *Comm. Pure Appl. Math.*, 59(6):797–829, 2006.
- [22] M. F. Duarte, M. A. Davenport, D. Takhar, J. N. Laska, T. Sun, K. F. Kelly, and R. G. Baraniuk. Single-pixel imaging via compressive sampling. *IEEE Signal Proc. Mag.*, 25(2):83–91, 2008.

- [23] H. Garudadri, P. K. Baheti, S. Majumdar, C. Lauer, F. Massé, J. van de Molengraft, and J. Penders. Artifacts mitigation in ambulatory ECG telemetry. In *The 12th IEEE International Conference on e-Health Networking, Applications and Services*, pages 338–344, 2010.
- [24] M. Genzel, G. Kutyniok, and M. März. ℓ^1 -analysis minimization and generalized (co-)sparsity: when does recovery succeed? *Appl. Comput. Harmon. Anal.*, 52:82–140, 2021.
- [25] M. Genzel, M. März, and R. Seidel. Compressed sensing with 1D total variation: breaking sample complexity barriers via non-uniform recovery. *Inf. Inference*, 11(1):203–250, 2022.
- [26] K. Gregor and Y. LeCun. Learning fast approximations of sparse coding. In *Proceedings of the 27th International Conference on Machine Learning*, pages 399–406, 2010.
- [27] J. Hou, X. Liu, H. Wang, and K. Guo. Tensor recovery from binary measurements fused low-rankness and smoothness. *Signal Process.*, 221:109480, 2024.
- [28] J. Hou, J. Wang, F. Zhang, and J. Huang. One-bit compressed sensing via ℓ_p ($0 < p < 1$)-minimization method. *Inverse Problems*, 36(5):055005, 35, 2020.
- [29] J. Huang, Y. Jiao, B. Jin, J. Liu, X. Lu, and C. Yang. A unified primal dual active set algorithm for nonconvex sparse recovery. *Stat. Sci.*, 36(2):215–238, 2021.
- [30] Y. Jiao, B. Jin, and X. Lu. A primal dual active set with continuation algorithm for the ℓ^0 -regularized optimization problem. *Appl. Comput. Harmon. Anal.*, 39(3):400–426, 2015.
- [31] B. Jin and P. Maass. Sparsity regularization for parameter identification problems. *Inverse Problems*, 28(12):123001, 70, 2012.
- [32] M. Kabanava and H. Rauhut. Analysis ℓ_1 -recovery with frames and Gaussian measurements. *Acta Appl. Math.*, 140:173–195, 2015.
- [33] M. Kabanava, H. Rauhut, and H. Zhang. Robust analysis ℓ_1 -recovery from Gaussian measurements and total variation minimization. *European J. Appl. Math.*, 26(6):917–929, 2015.
- [34] K. Li, H. Li, R. H. Chan, and Y. Wen. Selecting regularization parameters for nuclear norm-type minimization problems. *SIAM J. Sci. Comput.*, 44(4):A2204–A2225, 2022.
- [35] X. Li, L. Mo, X. Yuan, and J. Zhang. Linearized alternating direction method of multipliers for sparse group and fused LASSO models. *Comput. Statist. Data Anal.*, 79:203–221, 2014.
- [36] X. Li, D. Sun, and K.-C. Toh. On efficiently solving the subproblems of a level-set method for fused lasso problems. *SIAM J. Optim.*, 28(2):1842–1866, 2018.
- [37] J. Liu and X. Chen. ALISTA: Analytic weights are as good as learned weights in LISTA. In *International Conference on Learning Representations (ICLR)*, 2019.
- [38] J. Liu, L. Yuan, and J. Ye. An efficient algorithm for a class of fused lasso problems. In *Proceedings of the 16th ACM SIGKDD International Conference on Knowledge Discovery and Data Mining*, pages 323–332, 2010.
- [39] X. Liu, J. Peng, J. Hou, Y. Wang, and W. Jianjun. Guaranteed matrix recovery using weighted nuclear norm plus weighted total variation minimization. *Signal Process.*, 227:109706, 2025.
- [40] M. Lustig, D. Donoho, and J. M. Pauly. Sparse MRI: The application of compressed sensing for rapid MR imaging. *Magnetic Res. Med.*, 58(6):1182–1195, 2007.
- [41] Q. Mo and Y. Shen. A remark on the restricted isometry property in orthogonal matching pursuit. *IEEE Trans. Inform. Theory*, 58(6):3654–3656, 2012.
- [42] M. Mohammadi. A compact neural network for fused lasso signal approximator. *IEEE Trans. Cybern.*, 51(8):4327–4336, 2019.
- [43] V. Monga, Y. Li, and Y. C. Eldar. Algorithm unrolling: interpretable, efficient deep learning for signal and image processing. *IEEE Signal Proc. Mag.*, 38(2):18–44, 2021.
- [44] G. B. Moody and M. R. G. The impact of the MIT-BIH arrhythmia database. *IEEE Eng. Med. Biol. Mag.*, 20(3):45–50, 2001.
- [45] J.-J. Moreau. Proximité et dualité dans un espace hilbertien. *Bull. Soc. Math. France*, 93:273–299, 1965.

- [46] F. Rapaport, E. Barillot, and J. Vert. Classification of arrayCGH data using fused SVM. *Bioinformatics*, 24(13):i375–i382, 2008.
- [47] R. T. Rockafellar. *Convex analysis*, volume No. 28 of *Princeton Mathematical Series*. Princeton University Press, Princeton, NJ, 1970.
- [48] M. Scetbon, M. Elad, and P. Milanfar. Deep K-SVD denoising. *IEEE Trans. Imag. Proc.*, 30:5944–5955, 2021.
- [49] J. Sulam, A. Aberdam, A. Beck, and M. Elad. On multi-layer basis pursuit, efficient algorithms and convolutional neural networks. *IEEE Trans. Pattern Anal. Mach. Intell.*, 42(8):1968–1980, 2020.
- [50] L. Tang and P. X. K. Song. Fused lasso approach in regression coefficients clustering—learning parameter heterogeneity in data integration. *J. Mach. Learn. Res.*, 17:Paper No. 113, 23, 2016.
- [51] R. Tibshirani, M. Saunders, S. Rosset, J. Zhu, and K. Knight. Sparsity and smoothness via the fused lasso. *J. R. Stat. Soc. Ser. B Stat. Methodol.*, 67(1):91–108, 2005.
- [52] J. A. Tropp. Convex recovery of a structured signal from independent random linear measurements. In *Sampling theory, a renaissance*, Appl. Numer. Harmon. Anal., pages 67–101. Birkhäuser/Springer, Cham, 2015.
- [53] R. Vershynin. *High-dimensional probability*, volume 47 of *Cambridge Series in Statistical and Probabilistic Mathematics*. Cambridge University Press, Cambridge, 2018. An introduction with applications in data science, With a foreword by Sara van de Geer.
- [54] J. Wang, W. Fan, and J. Ye. Fused lasso screening rules via the monotonicity of subdifferentials. *IEEE Trans. Pattern Anal. Mach. Intell.*, 37(9):1806–1820, 2015.
- [55] J. Wang, J. Huang, F. Zhang, and W. Wang. Group sparse recovery in impulsive noise via alternating direction method of multipliers. *Appl. Comput. Harmon. Anal.*, 49(3):831–862, 2020.
- [56] J. Wang, F. Zhang, J. Huang, W. Wang, and C. Yuan. A nonconvex penalty function with integral convolution approximation for compressed sensing. *Signal Process.*, 158:116–128, 2019.
- [57] W. Wang, F. Zhang, and J. Wang. Low-rank matrix recovery via regularized nuclear norm minimization. *Appl. Comput. Harmon. Anal.*, 54:1–19, 2021.
- [58] J. Wen, D. Li, and F. Zhu. Stable recovery of sparse signals via l_p -minimization. *Appl. Comput. Harmon. Anal.*, 38(1):161–176, 2015.
- [59] J. Wen, Z. Zhou, J. Wang, X. Tang, and Q. Mo. A sharp condition for exact support recovery with orthogonal matching pursuit. *IEEE Trans. Signal Process.*, 65(6):1370–1382, 2017.
- [60] Y.-W. Wen and R. H. Chan. Parameter selection for total-variation-based image restoration using discrepancy principle. *IEEE Trans. Image Process.*, 21(4):1770–1781, 2012.
- [61] B. Xin, Y. Kawahara, Y. Wang, and W. Gao. Efficient generalized fused lasso and its application to the diagnosis of alzheimer’s disease. In *Proceedings of the 28-th AAAI Conference on Artificial Intelligence*, volume 28, pages 2163–2169, 2014.
- [62] Y. Yang, J. Sun, H. Li, and Z. Xu. ADMM-CSNet: a deep learning approach for image compressive sensing. *IEEE Trans. Pattern Anal. Mach. Intell.*, 42(3):521–538, 2020.
- [63] G.-B. Ye and X. Xie. Split Bregman method for large scale fused Lasso. *Comput. Statist. Data Anal.*, 55(4):1552–1569, 2011.
- [64] Y. Zhang, Y. Shen, R. Zhang, Y. Liu, Y. Guo, D. Deng, and I. D. Dinov. Numerical methods for computing the discrete and continuous Laplace transforms. Preprint, arXiv:2304.13204, 2023.